AD-A042 104 NAVAL POSTGRADUATE SCHOOL MONTEREY CALIF F/G 1/3
WING ROCK AS A LATERAL-DIRECTIONAL AIRCRAFT LIMIT CYCLE OSCILLA--ETC(U)
JUN 77 P D YOUNG

UNCLASSIFIED NL

| OF |
AD
A042104

END

DATE
FILMED
8-77

(2)
B.S

NAVAL POSTGRADUATE SCHOOL
Monterey, California

THESIS

WING ROCK AS A LATERAL-DIRECTIONAL AIRCRAFT LIMIT CYCLE OSCILLATION INDUCED BY NONLINEAR AERODYNAMICS OCCURRING AT HIGH ANGLE OF ATTACK

by

Paul D. Young

June 1977

Thesis Advisor: L. V. Schmidt

Approved for public release; distribution unlimited.

Unclassified

SECURITY CLASSIFICATION OF THIS PAGE (When Data Entered)

REPORT DOCUMENTATION PAGE

READ INSTRUCTIONS BEFORE COMPLETING FORM

1. REPORT NUMBER

2. GOVT ACCESSION NO.

3. RECIPIENT'S CATALOG NUMBER

4. TITLE (and Subtitle)
Wing Rock as a Lateral-Directional Aircraft Limit Cycle Oscillation Induced by Nonlinear Aerodynamics Occurring at High Angle of Attack.

5. TYPE OF REPORT & PERIOD COVERED
Master's Thesis; June 1977

6. PERFORMING ORG. REPORT NUMBER

7. AUTHOR(s)
Paul David Young

8. CONTRACT OR GRANT NUMBER(s)

9. PERFORMING ORGANIZATION NAME AND ADDRESS
Naval Postgraduate School
Monterey, California 93940

10. PROGRAM ELEMENT, PROJECT, TASK AREA & WORK UNIT NUMBERS

11. CONTROLLING OFFICE NAME AND ADDRESS
Naval Postgraduate School
Monterey, California 93940

12. REPORT DATE
June 1977

13. NUMBER OF PAGES
174

14. MONITORING AGENCY NAME & ADDRESS(if different from Controlling Office)
Naval Postgraduate School
Monterey, California 93940

15. SECURITY CLASS. (of this report)
Unclassified

15a. DECLASSIFICATION/DOWNGRADING SCHEDULE

16. DISTRIBUTION STATEMENT (of this Report)
Approved for public release; distribution unlimited.

17. DISTRIBUTION STATEMENT (of the abstract entered in Block 20, if different from Report)

18. SUPPLEMENTARY NOTES

19. KEY WORDS (Continue on reverse side if necessary and identify by block number)
Wing Rock as a Limit Cycle Oscillation
Lateral-Directional Motion at High Angle of Attack
Hysteresis Induced Wing Rock
Nonlinear Aerodynamics and Wing Rock
Limit Cycle Oscillations in Aircraft

20. ABSTRACT (Continue on reverse side if necessary and identify by block number)
Wing rock at high angle of attack is an oscillatory lateral-directional motion phenomenon known to exist in some of today's high performance tactical aircraft. The motion has been consistently characterized as a lightly damped Dutch-Roll oscillation attributable to asymmetric wing stall. However, evidence gathered from wind tunnel simulations and at least one British study indicate that aerodynamic
NEXT Page

DD FORM 1 JAN 73 1473 EDITION OF 1 NOV 68 IS OBSOLETE
S/N 0102-014-6601

Unclassified

SECURITY CLASSIFICATION OF THIS PAGE (When Data Entered)

nonlinearities may be the source of wing rock. Regardless of the actual cause of the phenomenon, a study of wing rock has positive ramifications with respect to gaining a clearer understanding of the aerodynamics associated with high angle of attack flight. This report presents the results of an investigation of wing rock which centered on the premise that two distinct nonlinear aerodynamic mechanisms (aerodynamic hysteresis and a cubic nonlinearity in yawing moment) not only can cause wing rock but may drive it to a limit cycle oscillation as well.

Approved for public release; distribution unlimited.

Wing Rock as a Lateral-Directional Aircraft Limit Cycle Oscillation Induced by Nonlinear Aerodynamics Occurring at High Angle of Attack

by

Paul David Young
Major, U.S. Marine Corps
B.S., Chemistry, Oklahoma State University, 1964

Submitted in partial fulfillment of the
requirements for the degree of

MASTER OF SCIENCE IN AERONAUTICAL ENGINEERING

from the

NAVAL POSTGRADUATE SCHOOL

June 1977

Author Paul D Young

Approved by: Louis V. Schmidt
Thesis Advisor

Second Reader

Chairman, Department of Aeronautics

Dean of Science and Engineering

ABSTRACT

Wing rock at high angle of attack is an oscillatory lateral-directional motion phenomenon known to exist in some of today's high performance tactical aircraft. The motion has been consistently characterized as a lightly damped Dutch-Roll oscillation attributable to asymmetric wing stall. However, evidence gathered from wind tunnel simulations and at least one British study indicate that aerodynamic nonlinearities may be the source of wing rock. Regardless of the actual cause of the phenomenon, a study of wing rock has positive ramifications with respect to gaining a clearer understanding of the aerodynamics associated with high angle of attack flight. This report presents the results of an investigation of wing rock which centered on the premise that two distinct nonlinear aerodynamic mechanisms (aerodynamic hysteresis and a cubic nonlinearity in yawing moment) not only can cause wing rock but may drive it to a limit cycle oscillation as well.

TABLE OF CONTENTS

LIST OF FIGURES

LIST OF SYMBOLS

b = Wing span

C_l = Dimensionless rolling moment coefficient = (R.M.)/qSb

C_n = Dimensionless yawing moment coefficient = (Y.M.)/qSb

I = Mass moment of inertia. Subscript x, y or z denotes reference body axis.

L = (Rolling Moment)/I_x, positive tends to lower right wing.

N = (Yawing Moment)/I_z, positive tends to yaw right wing aft.

p = Roll rate $d\phi/dt$ (or $\dot{\phi}$)

q = Dynamic pressure, $\frac{1}{2}\rho U^2$.

r = Yaw rate = $d\psi/dt$ (or $\dot{\psi}$)

S = Wing area

T = Period of motion ($2\pi/\omega$)

U = Freestream velocity

Greek Symbols:

β = Sideslip angle, positive for wind vector coming from the right.

ϕ = Bank angle, positive for right wing down.

ψ = Yaw angle, positive for nose moving to the right.

φ = Phase angle

ζ = Dimensionless damping ratio

ϵ = Dimensionless nonlinearity variable

σ = Sideslip amplitude term

λ = Eigenvalue or ratio of $\dot{\sigma}/\sigma$ as noted in text usage

ρ = Atmospheric density

δ_a = Aileron deflection

$\Delta( )$ = Incremental change of a variable

ω = Circular frequency

(ω_n = undamped natural frequency)

($\omega_d = \sqrt{1 - \zeta^2}\ \omega_n$ = damped natural frequency)

Subscripts:

$( )_\beta$ = $\partial( )/\partial\beta$, partial derivative with respect to sideslip angle

$( )_p$ = $\partial( )/\partial\ pb/2U$

$( )_r$ = $\partial( )/\partial\ rb/2U$

Time Derivative:

$(\dot{})$ = $d( )/dt$

ACKNOWLEDGEMENT

I wish to express my sincere gratitude to Professor Louis V. Schmidt for stimulating my interest and serving in a patient, dedicated and untiring manner as my thesis advisor.

My thanks also to Professor Arthur Schoenstadt of the Mathematics Department for providing needed assistance in overcoming mathematical and computer programming difficulties that arose during the course of the research.

I. INTRODUCTION

Wing rock at moderate to high angle of attack is a characteristic known to exist in some of today's high performance aircraft, particularly those possessing the characteristics of thin swept wings and a slender fuselage. The terminology "wing rock" has been used to characterize an oscillatory lateral-directional motion exhibited by some aircraft when operating near stall, or when flow separation is evident by airframe buffeting. Although the motion has been observed and documented extensively during flight tests, its exact cause has remained essentially unknown. In an attempt to explain wing rock, fleet aviators, test pilots and aerodynamicists have consistently advanced the theory which has generally concluded that the apparent random rolling moments manifested by alternating wing rock motion at or near stall are due to asymmetric spanwise loading, i.e., alternating stall condition along the wing span. It is not the intent of this thesis to dispute such arguments but rather to present new arguments based on the premise that aerodynamic nonlinearities may not only cause wing rock but may drive it to a limit cycle oscillation.

A. PAST EXPERIENCE WITH WING ROCK

The author has had experience as a test pilot at the Naval Air Test Center and has personally observed what could be essentially described as a wing rock limit cycle while

conducting high angle of attack flight tests with the Northrop T-38A airplane. The T-38A is control limited longitudinally to the extent that it can not be made to achieve the so-called "classic aerodynamic stall", i.e., complete flow separation along the wing span. As a result, the normal 1-g stall is defined when a maximum angle of attack is reached due to control-limiting, moderate-to-heavy airframe buffet and a wing rock motion are evident with an average amplitude excursion in bank angle of $\pm$ 20 degrees. This lateral motion occurs with essentially no heading deviation and will continue indefinitely, albeit accompanied by a large sink rate, until the angle of attack is reduced. The buffeting and wing rock will immediately cease and a complete recovery can be effected with very little additional loss of altitude, when afterburner thrust is applied.

The question of whether wing rock motion in the T-38 (F-5 series probably behaves the same) is indeed a limit cycle oscillation caused by aerodynamic phenomena other than asymmetric spanwise loading has never really been seriously considered from a flight test standpoint. Instead, most test pilots and engineers associated with experimental/developmental flight testing quickly assume that an asymmetric stall condition is responsible, since the motion is typically accompanied by separation as evidenced by airframe buffeting. Most swept wing aircraft exhibit wing rock motion to one degree or another near stall, although few can actually be said to exhibit motion behaving as a limit cycle. Since most aircraft are not control

limited, the approach to stall will often continue past that point where an oscillation similar to that exhibited by the T-38 might occur. The Vought A-7 and F-8 series are notable examples of aircraft that can quickly reach a point where directional stability is lost, resulting in an almost immediate departure from controlled flight, if the pilot does not respond quickly enough to reduce the angle of attack.

Informal liaison with NASA Langley revealed that free flight model testing of the T-38A had on at least one occasion confirmed the existence of a wing rock limit cycle. Although credibility of this report would have been enhanced had it been possible to conduct an analysis of lateral directional motion at high angle of attack on a current production aircraft such as the T-38 or F5, the necessary information needed to conduct such an analysis was not forthcoming owing to proprietary considerations. Thus, it was necessary to investigate and illustrate the concept of a wing rock limit cycle using the textbook airplane, F-94, as presented in Blakelock [Ref. 1]. During the course of the research the stability derivatives of the production F-94 were modified as necessary to simulate desired test conditions. To the extent that the F-94 served as a vehicle with which to demonstrate the concept of wing rock as a limit cycle, it was a satisfactory substitute in lieu of a current production aircraft.

B. A NEW THEORY PROPOSED

Explaining wing rock as an aerodynamic phenomenon apart from the theory of asymmetric wing stall poses some difficulty

partly from the fact that the motion closely resembles a lightly damped Dutch-Roll oscillation. Evidence obtained from closely controlled wind tunnel experiments [Ref. 2] and observations made during flight tests seem to suggest the possibility of a limit cycle oscillation wherein the amplitude and period of the motion may result solely from nonlinear aerodynamics. This contrasts with the response of a lightly damped Dutch-Roll oscillation where the amplitudes are a function of the initial conditions.

Some difficulty arises when attempting to identify an aerodynamic nonlinearity that may contribute to wing rock motion in wind-tunnel or flight tests since most dynamic analysis techniques, including aircraft parameter identification, are oriented towards a linearized model of the aircraft. Presumably, a nonlinear model could be assumed for parameter identification purposes but a question of uniqueness would arise since several completely different plant models might produce equally valid time history matches with actual flight data. Therefore, a significant step at this time would be the recognition of wing rock motion as a limit cycle oscillation induced by aerodynamic nonlinearities.

Ross [Ref. 3], has shown that a wing rock limit cycle can exist when a nonlinearity of cubic form is present in either yawing or rolling moment with respect to sideslip angle. Ross used the Krylof-Bogoliubof method (KB method) with the assumption of slowly varying parameters to analyze the mathematical model of the motion described by the test airplane.

A portion of the analysis presented herein explores further the work done by Ross with the objective of obtaining a simplified form of the theory she proposed as well as amplifying upon it. Preceding this, however, will be an analysis and discussion designed to support the claim that a wing rock limit cycle may also be the result of a nonlinear mechanism referred to as aerodynamic hysteresis.

C. MOTIVATION

The study of wing rock and its causes has direct application to an analysis of stall and post-stall gyrations which have long been difficult to predict and control on many tactical aircraft. The Vought F-8 and A-7 are notable examples. Increased knowledge in this area would surely enhance the ability to predict aerodynamic behavior, thus enabling an earlier detection of undesirable flying qualities, or design improvement or, at least, a minimization of mission limiting or annoying characteristics.

II. METHOD OF INVESTIGATION AND EQUIPMENT USED

The investigation of wing rock involved the use of the EAI (Electronics Associates Incorporated) model 580 analog computer as well as the Naval Postgraduate School's Department of Aeronautics digital computing facilities, namely, the Hewlett Packard, HP-9830. Mathematical models representing the pertinent equations of motion were programmed on, and results compared from, both machines to ensure validity of programming. The output from these computing machines consisted of time histories of the motion exhibited by the test aircraft (F-94) when released from some initial condition. Output data were recorded by a graphical plotter or strip chart recorder attached as a peripheral device to the main computing units. These time history plots were used to make both qualitative and quantitative assessements of the motion, including measurements of critical damping ratio, frequency and/or period. Digital as well as graphical output was obtained using the HP-9830. Time history plots appearing herein were initially made using the analog computer, but final copies were obtained from the HP-9830 plotter as it produced a more compatible form for this report. The analog computer was superior to the digital machine in terms of its ease of programming or modification of the program during execution where it was possible to view readily the effects of altering certain key aircraft parameters.

The mathematical model used for laboratory tests consisted of the linearized lateral-directional equations of motion with certain simplifications to be presented later. As mentioned earlier, the F-94 airplane as presented in detail in Blakelock [Ref. 1] was used as the test vehicle for conducting laboratory simulations of wing rock motion. In its production configuration the airplane exhibits no inherent instabilities with respect to the lateral-directional modes of motion. Modifications were made to its production stability derivatives as necessary to conduct desired simulations.

III. RESULTS AND DISCUSSION

The discussion will focus on the particular lateral-directional motion exhibited by some aircraft within their respective flight envelopes and referred to hereafter as wing rock. The first part of this section will be devoted to a presentation of the analysis and investigation of wing rock as a limit cycle induced by aerodynamic hysteresis. The second part will present a similar analysis and investigation of wing rock as a limit cycle induced by a natural instability in the aircraft that is constrained by a nonlinearity in one or more stability derivatives. The reader is advised to refer to pages 8 and 9 for definitions of symbology used throughout the following discussion.

A. THE GENERAL LIMIT CYCLE OSCILLATION

A limit cycle oscillation is similar physically to the motion described by the typical undamped harmonic oscillator represented by:

$$\ddot{X} + \alpha X = 0$$

which has solution:

$$x(t) = A \sin(\sqrt{\alpha}\, t + \phi)$$

$$\dot{x}(t) = A\sqrt{\alpha} \cos(\sqrt{\alpha}\, t + \phi)$$

The motion amplitude of the linear undamped system will depend upon the initial conditions, and hence different initial conditions will result in different amplitude histories.

The linear undamped system will, of course, exhibit no damping behavior of the motion. By contrast, a nonlinear system that demonstrates a limit cycle behavior will have the same amplitude description for motion regardless of the initial conditions. A system that is weakly nonlinear with a limit cycle behavior will appear to have the properties of a linear system; however, the characteristic of motion amplitude regardless of initial condition is a distinctly different attribute of the nonlinear system. One should recognize that the above differences are somewhat heuristic and a mathematician would characterize the distinctions with considerably more detail.

B. AERODYNAMIC HYSTERESIS

Wind-tunnel tests on aircraft models often show that the rolling moments measured on a symmetric model, when yaw angle is zero and angle of attack is increased, are approximately zero-valued until the angle of attack approaches close to stall. Rolling moments tend to be erratic at or near stall, and it is customary to attribute these traits to slight asymmetries in the model or tunnel flow, with a resulting early stall of one wing relative to the other. A recent wind-tunnel test [Ref. 2] upon a sting-mounted model having a strain gage balance with appropriate electronic filtering, used the test technique of conducting a slow, continuous yaw angle sweep through a complete cycle of yaw motion. When the cyclic yaw sweep was conducted at or near stall angle, both rolling and yawing moments showed incremental shifts in value that appeared to be related to the direction of the slow yaw sweep.

The curves of rolling moment, when plotted versus yaw angle, gave evidence of aerodynamic hysteresis.

Simply stated, aerodynamic hysteresis is a type of behavior wherein an aircraft's response to a given input is such that it does not follow the same path returning to equilibrium as it did when initially displaced. Of importance here is the fact that the aircraft remains positively stable. Figure 1 is an illustration of stall hysteresis wherein the airplane experiences a sudden decrease in lift coefficient as a result of complete flow separation along the wing span at stall angle of attack. The airplane recovers to a lower lift coefficient and angle of attack only to repeat the cycle if the controls are held in a pro-stall condition. This type of motion is often referred to as "stall porpoising" and is common to most aircraft with high aspect ratio wings. This example of longitudinal hysteresis is presented to the reader as an aid in understanding the discussion to follow pertaining to lateral-directional hysteresis.

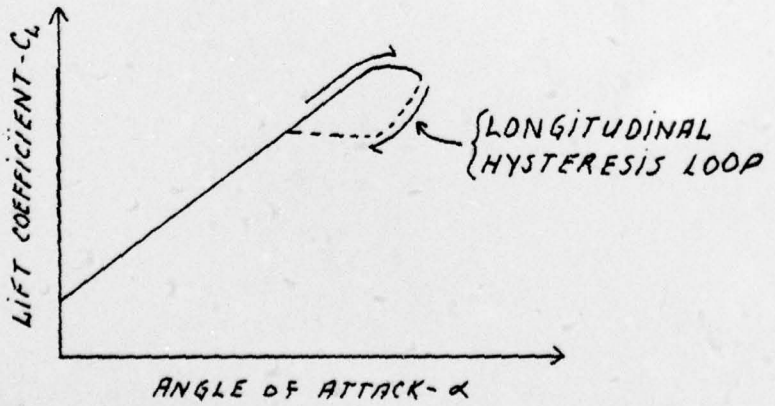

Figure 1. Stall porpoising and longitudinal hysteresis.

1. Theory

The analysis presented here will include some simplifications where deemed appropriate. The interest is to use state variable format to represent the mathematical model of the pertinent lateral-directional motion. The state variable format will be extended in an illustrative sense to demonstrate a wing rock limit cycle due to aerodynamic hysteresis. It is assumed that the lateral-directional motion of the aircraft occurs in such a manner that the airplane remains on a straight flight path, hence yaw and sideslip angles are related by:

$$\psi = -\beta \tag{1}$$

Further, it is assumed that the aircraft is operating at a fixed angle of attack with all control surfaces fixed. Therefore,

$$\dot{r} I_z = \sum \text{yawing moment}$$
$$= \bar{q} S b \left[C_{n_\beta} \beta + \frac{b}{2U} \left(C_{n_r} r + C_{n_p} p \right) \right] \tag{02a}$$

and

$$\dot{p} I_x = \sum \text{rolling moment}$$
$$= \bar{q} S b \left[C_{l_\beta} \beta + \frac{b}{2U} \left(C_{l_r} r + C_{l_p} p \right) \right] \tag{02b}$$

Since $r = \frac{d\psi}{dt} = -\frac{d\beta}{dt} = -\dot{\beta}$ and $\dot{r} = -\ddot{\beta}$ equations (02a) and (02b) can be simplified to:

$$\ddot{\beta} = -N_\beta \beta + N_r \dot{\beta} - N_p p \tag{03a}$$

and

$$\dot{p} = L_\beta \beta - L_r \dot{\beta} - L_p p \tag{03b}$$

Further modifications have been made yielding a dimensional form of the linearized lateral-directional equations of motion. The assumption that a straight flight path is maintained effectively eliminates any influence from sideforces and the usual accompanying spiral mode. Such an assumption is reasonable and consistent with flight test observations of wing rock motion.

The freely vibrating system represented mathematically in equations (03) may be cast into state variable format as:

$$\{\dot{x}\} = [A]\{x\}$$

which corresponds to the shorthand notation for the following:

$$\begin{Bmatrix} \dot{\beta} \\ \ddot{\beta} \\ \dot{p} \end{Bmatrix} = \begin{bmatrix} 0 & 1 & 0 \\ -N_\beta & N_r & -N_p \\ L_\beta & -L_r & L_p \end{bmatrix} \begin{Bmatrix} \beta \\ \dot{\beta} \\ p \end{Bmatrix} \qquad (04)$$

A third equation or identity $\beta \equiv \dot{\beta}$ is necessary to accommodate all the state variables in the matrix format.

To digress briefly, $\{x\}$ represents the state vector which contains the components of sideslip angle, β, sideslip velocity, $\dot{\beta}$, and roll rate, p. The plant matrix $[A]$ is of order 3 and contains the dimensional stability derivatives (standard NASA convention) which resulted from the previous analysis. These derivatives are explicitly defined as follows:

$$a_{11} = a_{13} = 0 \; ; \qquad a_{12} = 1$$

$$a_{21} = -N_\beta = \frac{-qSb}{I_z} C_{n_\beta}$$

$$a_{22} = N_r = \frac{\bar{q}Sb^2}{2I_z U} C_{n_r} \qquad a_{32} = -L_r = \frac{-\bar{q}Sb^2}{2I_x U} C_{l_r}$$

$$a_{23} = -N_p = \frac{-\bar{q}Sb^2}{2I_z U} C_{n_p} \qquad a_{33} = -L_p = \frac{\bar{q}Sb^2}{2I_x U} C_{l_p}$$

$$a_{31} = L_\beta = \frac{\bar{q}Sb}{I_x} C_{l_\beta}$$

Equation (04) represents an eigenvalue problem of a freely vibrating system in which the eigenvectors are the modes of motion and the eigenvalues contain the corresponding characteristics of damping, natural frequency, and period. In its present linear form the system described by equation (04) has a solution consisting of three roots (one real and one complex conjugate pair) corresponding to the roll convergence (subsidence) and Dutch-Roll modes respectively. Again, making use of the state variable format the solution to the freely vibrating system may be expressed as:

$$\{x(t)\} = [\phi(t)] \{x(0)\} \qquad (05)$$

where $[\phi(t)]$ is the state transition matrix and $\{x(0)\}$ is the vector of values for the state variables at time equal to zero. In essence, the state transition matrix is used for modal analysis to project or propagate the aircraft's motion numerically from some starting values (initial condition) to another set of values at a specified time greater than zero.

The equations of motion for the dynamic system with control applied is given by:

$$\{\dot{x}\} = [A]\{x\} + [B]\{u\} \qquad (06)$$

where the control matrix [B] contains the control power derivatives for yawing and rolling moments associated with the aileron and rudder controls. The vector $\{u\}$ contains the magnitudes of the inputs for the respective controls. The general solution to equation (06) is expressed as:

$$\{x(t)\} = [\phi(t)]\{x(0)\} + [\phi(t)]\int_0^t [\phi(-\tau)][B]\{u(\tau)\}\,d\tau \qquad (07)$$

where the integral term is a convolution integral. This is a general solution in the sense that it applies to any of the standard input methods, i.e., step, ramp and impulse. The analysis and experimentation to which this section of theory applies was restricted to the case of step inputs, which is probably the most common control input method used in aerodynamics for studying aircraft dynamic stability.

The specific solution to equation (06) for a step input of control is expressed as: [Ref. 4]

$$\{x(t)\} = [\phi(t)]\{x(0)\} + [A]^{-1}[\phi(t) - I][B]\{u\} \qquad (08)$$

where $[A]^{-1}$ and [I] are the plant inverse and identity matrices respectively.

Figure 2 contains a representative form of the aerodynamic hysteresis assumed in the analysis of rolling moment.

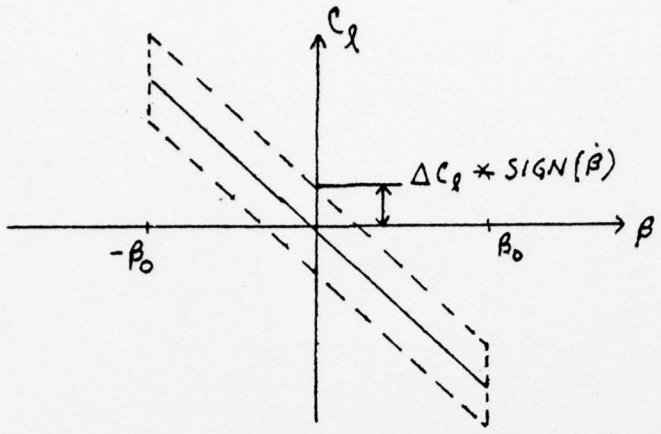

Figure 2. Assumed form of roll hysteresis.

The motion of the system corresponds to a periodic variation of the state variables such that the amplitude of the sideslip angle is assumed to be bounded by:

$$-\beta_o \leq \beta \leq \beta_o$$

Referring to figure 2, the hysteresis loop is defined by the dashed lines. The value of the rolling moment corresponding to a particular sideslip angle will be the sum of the production aircraft's linear roll-due-to sideslip and the additional hysteresis term, which has constant magnitude but varies in sign according to the sign of the sideslip velocity. This latter condition alludes to the manner in which the increment of rolling moment was applied, i.e., through a relay action mechanism ($\pm$) driven by the sign of sideslip velocity. Sideslip velocity will naturally be plus or minus in sign according to the direction of yaw, hence the increment of rolling moment was added or subtracted accordingly. Thus, the rolling moment due to sideslip as shown in Fig. 2 may be expressed as:

$$\text{Roll due to sideslip} = L(\beta) = L_\beta \beta + \Delta L * SIGN(\dot{\beta})$$

Figure 2 should not be construed to represent the only form that roll hysteresis may take but was used in this analysis to illustrate the concept. Nothing has been stated explicitly or implied up to this point with respect to the direction assumed by the hysteresis loop as the aircraft oscillates in yaw, i.e., clockwise or counter-clockwise, but this will be clarified later in the presentation of experimental results. Although not shown, yaw moment hysteresis may be assumed to be of similar form as that presented in Fig. 2.

In order to predict the behavior of the aircraft it was necessary to solve equation (08) after some simplifications required to facilitate the ease of computation were implemented. Under the assumption of a limit cycle, the motion is periodic and the amplitude remains constant, which can be expressed in part as:

$$\{x(t)\} = \{x(t+T)\}$$

where T is the period. Referring back to the column vector of state variables in equation (05) and with a convenient choice of the time origin:

$$X_2(0) = X_2(T/2) = x(T) = \dot{\beta} = 0$$

This is a necessary and sufficient condition to assure proper establishment of the relay action on roll moment hysteresis. The forcing function portion of equation (06) may be expressed as:

$$[B]\{u\} = \Delta L \begin{Bmatrix} 0 \\ \vdots \\ 1 \end{Bmatrix} \text{SIGN}(\dot{\beta}) \qquad (09)$$

where $\Delta L = \frac{qSb}{I_x} \Delta C_l$

The value of unity in vector element u(3) of equation (09) is used to denote a step input of the roll moment increment, ΔL. This can be equated to a step input of aileron by the pilot, though roll hysteresis should not be considered as having that as its source, in keeping with the requirement for this analysis that controls be fixed. An external source may, in fact, be the origin of roll hysteresis. Carrying the previous logic further, it is valid to consider the motion over a half-cycle since periodicity once again requires that:

$$\{X(T/2)\} = -\{X(0)\}$$

and $$X_2(0) = -X_2(T/2) = 0$$

Substituting these simplifications into equation (08) yields:

$$\{X(T/2)\} = \phi(T/2)\{x(0)\} + [A]^{-1}[\phi(T/2) - I][B]\{u\}\Delta L$$

$$-\{x(0)\} - \phi(T/2)\{x(0)\} = [A]^{-1}[\phi(T/2) - I][B]\{u\}\Delta L$$

$$-[I + \phi(T/2)]\{x(0)\} = [A]^{-1}[\phi(T/2) - I][B]\{u\}\Delta L$$

$$\{x(0)\} = -[I + \phi(T/2)]^{-1}[A]^{-1}[\phi(T/2) - I][B]\{u\}\Delta L \qquad (09)$$

Equation (09) can be solved for the period T by numerically iterating for the value of T/2 which will cause $X_2(0)$, side-slip velocity, to vanish. However, it is necessary first to solve for the state transition matrix $[\phi(\div)]$ in order that all values are known except T/2. Coincidental to computing

the period, the maximum values of the state variables $X_1(0)$ and $X_3(0)$ (sideslip angle and roll rate, respectively) were determined, since these necessarily occurred at the state point where $X_2(0)$ vanished. Computationally, this was a simpler method than integrating equation (07). A sample solution will be presented later. Upon examining equation (09) it should be noted that the period of the limit cycle in no way depends upon the sign of roll moment hysteresis; however, the amplitude of the state variables is a linear function of the magnitude of roll moment hysteresis, ΔL. The same procedure as outlined above could be applied to an analysis of yaw moment hysteresis.

2. Analysis

For reasons given earlier in the introduction, the F-94 airplane was chosen as the test vehicle for conducting laboratory simulations of wing rock motion. In addition to being in the landing configuration, the following pertinent data relative to the F-94 was obtained from Blakelock [Ref. 1]:

$U = 135$ mph $= 198$ fps
$q = 46.6$ psf
$S = 239$ ft^2
$b = 37.3$ ft
$Ix = 7.16 \times 10^3$ slug-ft^2
$Iz = 33.01 \times 10^3$ slug-ft^2
$C_{l_\beta} = -.0487$ RAD^{-1}
$C_{l_p} = -.450$ "
$C_{l_r} = .0278$ RAD^{-1}
$C_{l_{\delta a}} = -.0916$ "
$C_{n_\beta} = .105$ "
$C_{n_p} = -.053$ "
$C_{n_r} = -.210$ "

For these values the plant matrix of equation (04) became:

$$[A] = \begin{bmatrix} 0 & 1 & 0 \\ -1.3214 & .2491 & .0629 \\ -2.822 & -1.517 & -2.4557 \end{bmatrix} \qquad (10)$$

a. Numerical Predictions

The system of three first order, ordinary linear differential equations in (04) were solved by using the computer program subroutine BASMAT, listed and described in Melsa and Jones [Ref. 5]. The Standard Fortran IV code was translated into the BASIC program language code for adaptation of BASMAT to the HP-9830 digital mini-computer. The eigenvalues of equation (04) using the plant defined by equation (10) were:

$$\lambda_1 = a = -2.4473 \text{ SEC}^{-1}$$

$$\lambda_{2,3} = b \pm ic = -.12873 \pm 1.1755\, i \text{ SEC}^{-1}$$

These values contain characteristic information pertaining to the two modes of motion which the aircraft exhibited as a freely vibrating system, i.e., no hysteresis imposed. These two modes were the roll convergence and Dutch-Roll modes. The roll convergence mode is indicated by the single real root, λ_1, while the Dutch-Roll mode is represented by the remaining complex roots, $\lambda_{2,3}$. This information was needed for comparison with the motion solutions obtained when hysteresis was applied (to be presented later). The Dutch-Roll mode indicated the following characteristics with respect to period, frequency and damping of the stable motion.

$$\zeta\omega_N = 0.12873 \text{ sec}^{-1}$$

$$\omega_d = \sqrt{1-\zeta^2}\,\omega_N = 1.755 \text{ sec}^{-1}$$

Hence: $\zeta = 0.109$

$$\omega_n = 1.183 \text{ sec}^{-1}$$

$$T_d = 5.345 \text{ sec.}$$

These calculations show that the Dutch-Roll mode is indeed stable, as expected for the production aircraft, with a damping level and undamped natural frequency of 10.9% of critical and 1.183 rad/sec, respectively. The roll convergence mode was not considered further, since the primary interest was in the oscillatory mode of motion.

The state transition matrix, $[\phi(t)]$, was obtained likewise from BASMAT and is presented below.

$$[\phi(t)] = [R]e^{at} + [[F]\cos(ct) + [G]\sin(ct)]e^{bt} \qquad (11)$$

where

$$[R] = \begin{bmatrix} 0.0114 & 0.0012 & 0.0093 \\ -0.0279 & -0.0030 & -0.0228 \\ 1.2146 & 0.1318 & 0.9916 \end{bmatrix}$$

$$[F] = \begin{bmatrix} 0.9886 & -0.0012 & -0.0093 \\ 0.0279 & 1.0030 & 0.0228 \\ -1.2146 & -0.1318 & 0.0084 \end{bmatrix}$$

$$[G] = \begin{bmatrix} 0.1320 & 0.8531 & 0.0184 \\ -1.1791 & -0.1084 & 0.0086 \\ -0.0050 & -1.0305 & -0.0236 \end{bmatrix}$$

and a, b, c derived from $\lambda_1 = a$

$$\lambda_{2,3} = b \pm ic$$

With this information input to equation (09), and applying an iterative solution technique, the period and amplitudes of the state variables for the cases of imposing roll and yaw moment hysteresis either independently or concurrently was obtained. The results for varying values of roll and yaw moment hysteresis are presented in Table I.

TABLE I

Results of Numerical Solution of Eq. (09) for Different Magnitudes of Roll & Yaw Hysteresis

Type Hysteresis	Magnitude of Hysteresis	Max β (Radians)	Max $\dot{\varphi}$ (Rad/sec)	Period T (sec)
Roll	1	.0922	.2948	5.5977
Roll	2	.1844	.5897	5.5979
Yaw	.05	.2105	-.2551	5.3459
Yaw	.1	.4210	-.5102	5.3457
Roll	-1	-.0922	-.2948	5.5977
Roll (1) + Yaw	1 .05	.3007	.0419	5.4219
Roll (1) + Yaw	.03 .5	.1714	-4.514E-03	5.4121

(1) Only condition for which roll rate, $\dot{\varphi}$, is not a maximum. All other values are necessarily maximums.

The iterative solution technique of interval halving, as described by Gerald [Ref. 6] was used to solve Eq. (09) for the values in Table I. Two function values of opposite sign were initially obtained by inputing estimates of the period. Thus started, the interval halving routine converged in an iterative fashion to a solution. The computer program used for this purpose and implemented on the HP-9830 is presented in Appendix A.

The state transition matrix, with its linear combination of the eigenvectors (mode shapes), allowed identification of the individual parameters comprising the Dutch-Roll mode. This identification follows from equation (11) and the following trigonometric identity:

$$A \sin\theta + B \cos\theta \equiv K\left(\frac{A}{K}\sin\theta + \frac{B}{K}\cos\theta\right) \equiv K \sin(\theta + \varphi)$$

where

$K = A^2 + B^2$ = magnitude of motion vector in polar coordinates

φ = Arctan B/A = phase angle of motion vector in polar coordinates.

Applying this mathematical form to the second term on the right of equation (11) results in:

$$[F]_{i,j} \cos(ct) + [G]_{i,j} \sin(ct) \equiv K\left(\frac{A}{K}\sin\theta + \frac{B}{K}\cos\theta\right) \equiv K\sin(\theta+\varphi)$$

where $K_{i,j} = \left([F]_{i,j} + [G]_{i,j}\right)^{1/2}$ = magnitude of motion vector

and $\varphi_{i,j} = \text{Arctan}\ \dfrac{[F]_{i,j}}{[G]_{i,j}}$ = phase angle of motion vector

i,j = array locations.

Using this and appropriate initial conditions such that

$$\{x(0)\} = \begin{Bmatrix} \beta(0) \\ \dot{\beta}(0) \\ p(0) \end{Bmatrix} = \begin{Bmatrix} 1 \\ 0 \\ 0 \end{Bmatrix}$$

the resulting relative magnitudes and phase angles of the elements comprising the total Dutch-Roll motion vector when normalized with respect to sideslip angle were:

$$\{K\} = \begin{matrix} \beta = 1.00 \\ \dot{\beta} = 1.183 \\ p = 1.218 \\ \phi \approx 1.030 \end{matrix} \qquad \{\varphi\} = \begin{matrix} \varphi_\beta = 0.0 \text{ Deg.} \\ \varphi_{\dot{\beta}} = 96.25 \text{ Deg.} \\ \varphi_p = 187.38 \text{ Deg.} \\ \varphi_\phi \approx 91.13 \end{matrix}$$

Although bank angle was not a state variable, its value can be determined as a function of time according to the relationship $\phi(t) = \int_0^t p(t)\,dt$, or approximated by $\phi(t) = \frac{p(t)}{\omega_n}$. The integration approach was used on both the analog and digital computers. Bank angle was introduced to gain a better understanding of the motion's character, specifically with respect to the relative amplitude ratio of bank angle to sideslip angle. A positive value for the phase angle above indicates phase lead.

b. Verification of Numerical Predictions

The numerical computations presented in the foregoing were verified qualitatively by modeling the subject aircraft in the laboratory on the EAI-580 analog computer. The circuit required for the hysteresis model is shown in Appendix E. The same model using the system of equations given in equations (03) was programmed on the HP-9830 for the purpose

of obtaining quantitative data. Digital propagation of aircraft motion was obtained by a numerical time-solution of the differential equations using the Euler Predictor-Corrector method given in Ref. [6]. The computer program used on the HP-9830 for this purpose is presented in Appendix B. A separate program (Appendix C) for plotting output from the program in Appendix B was necessary to avoid overflowing available memory capacity due to large storage arrays used.

Time history plots of aircraft response are presented in figures 3 through 10. These computer generated plots were obtained by numerically integrating, as previously mentioned, the following governing equations of motion:

$$\ddot{\beta} = -N_\beta \beta + N_r \dot{\beta} - N_p p + \Delta N * SIGN(\dot{\beta})$$

$$\dot{p} = L_\beta \beta - L_r \dot{\beta} - L_p p + \Delta L * SIGN(\dot{\beta})$$

These are equations (03) with roll and yaw hysteresis terms added. The third equation contained in matrix equation (04) was merely an identity and thus served no useful purpose in performing numerical integration.

The time history responses in figures 3 through 6 are arranged to facilitate comparison of the characteristics of the two forms of motion, i.e., the damped Dutch-Roll and limit cycle oscillation. The Dutch-Roll mode was not duplicated on all plots; therefore, it will be necessary for the reader to refer back to figures 3 through 6 for comparison purposes. All of the time history data were plotted with sideslip angle as a reference parameter.

Figures 3 through 6 show the limit cycle resulting from the application of an increment of roll moment hysteresis

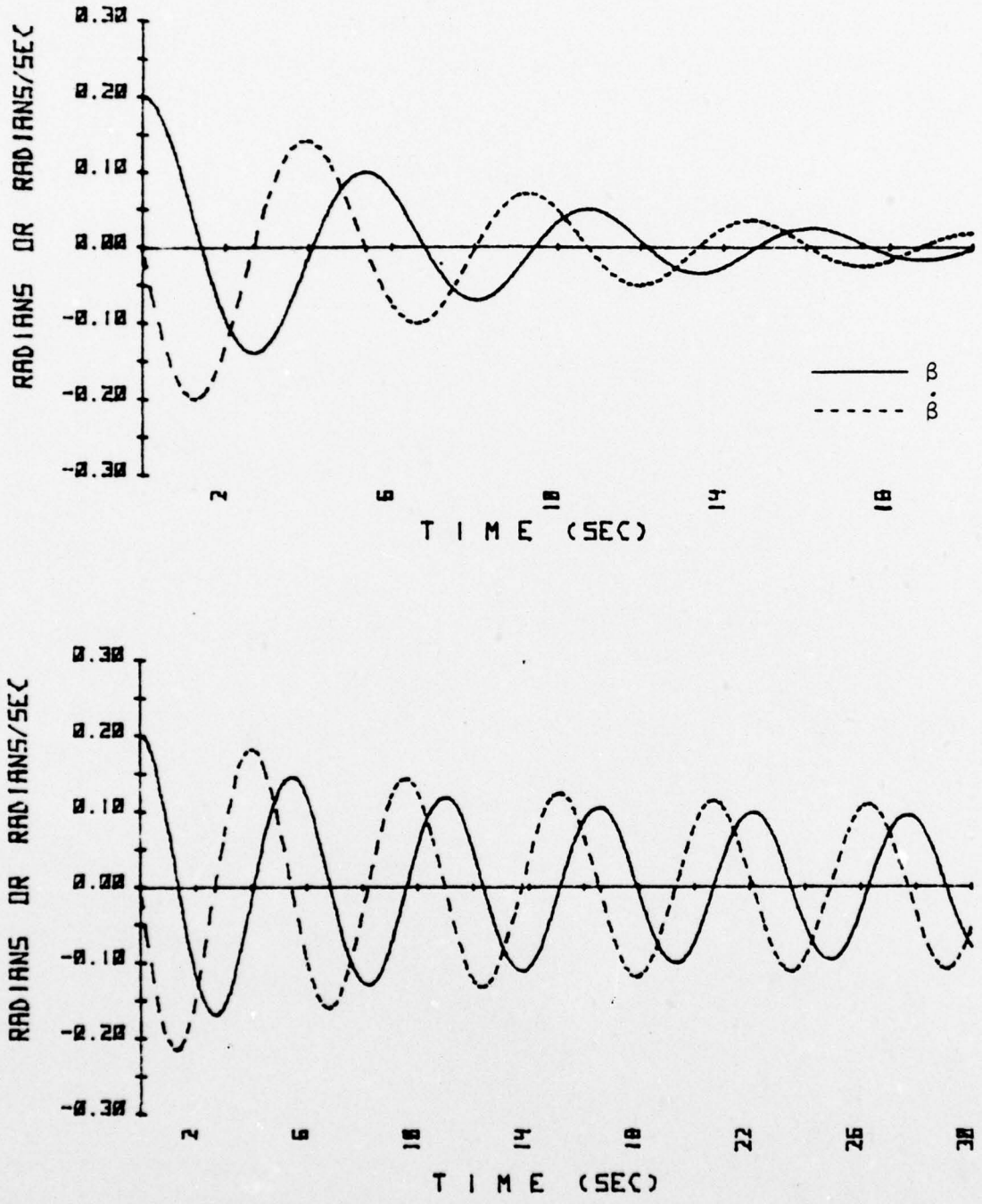

Figure 3. Stable Dutch-Roll (Upper Plot); Wing Rock Limit Cycle Induced by Roll Hysteresis (Lower Plot), β and $\dot{\beta}$ Comparison.

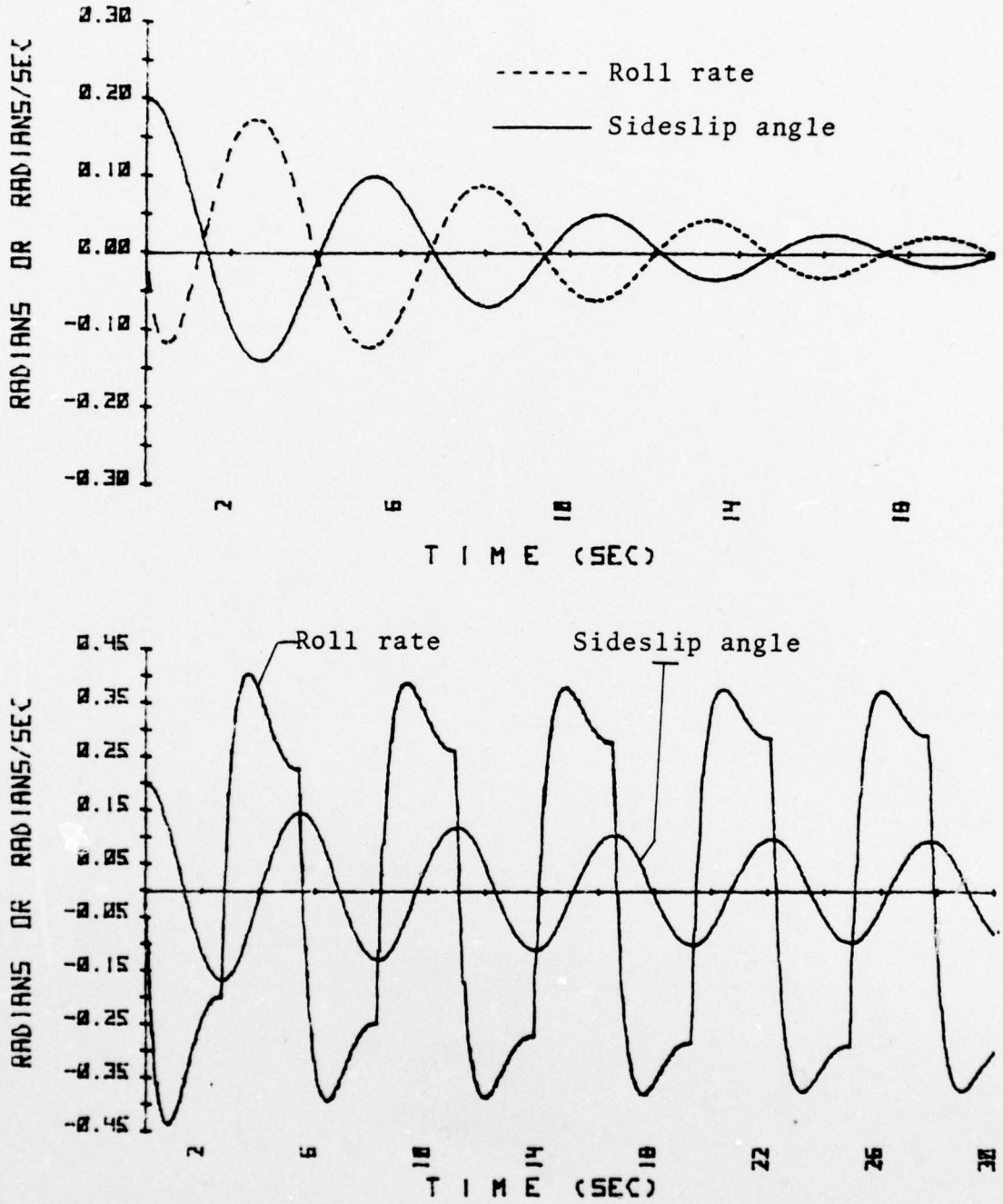

Figure 4. Stable Dutch-Roll (Upper Plot); Wing Rock Limit Cycle Induced by Roll Hysteresis (Lower Plot), β and p Comparison.

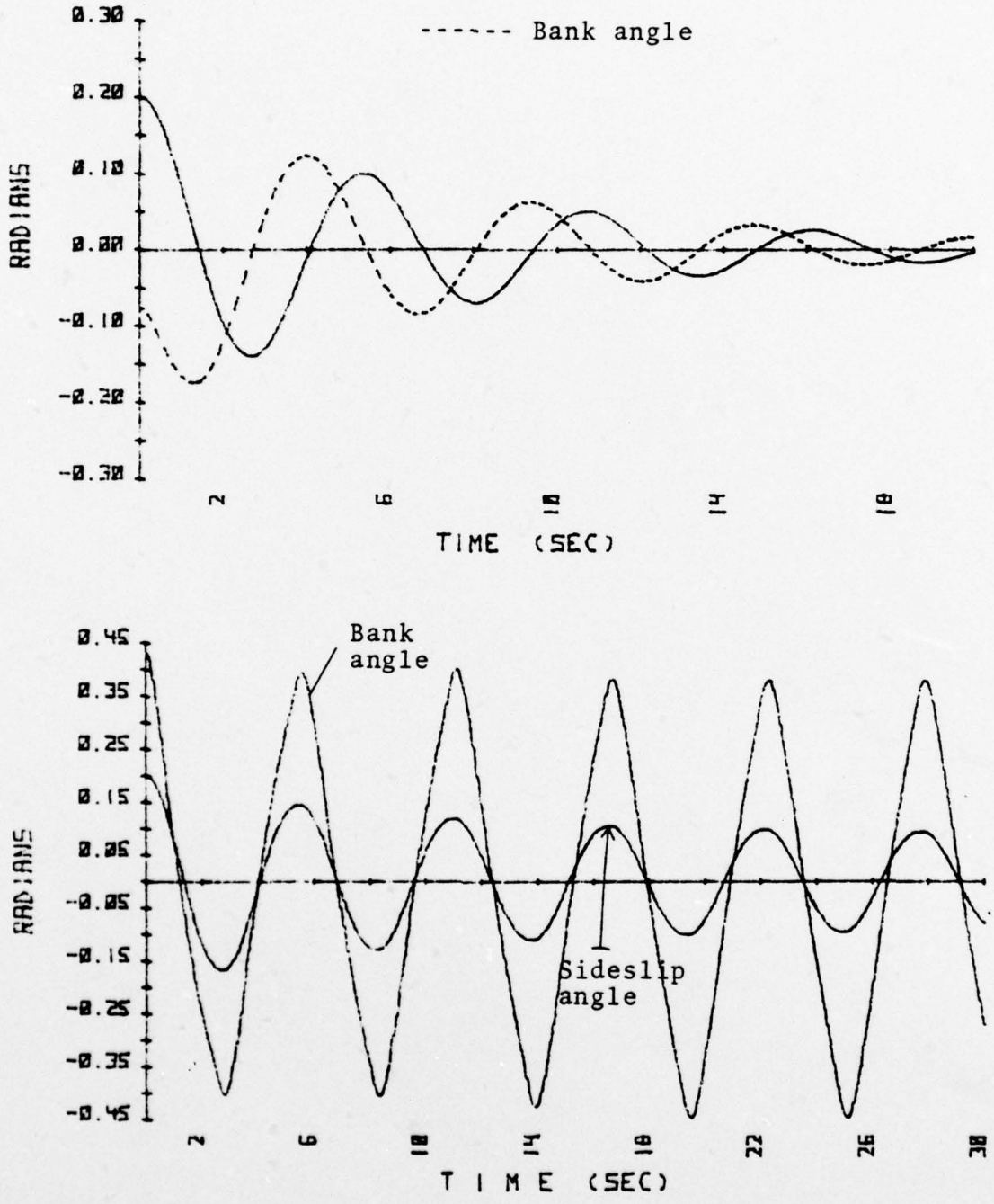

Figure 5. Stable Dutch-Roll (Upper Plot); Wing Rock Limit Cycle Induced by Roll Hysteresis (Lower Plot); β and ϕ Comparison.

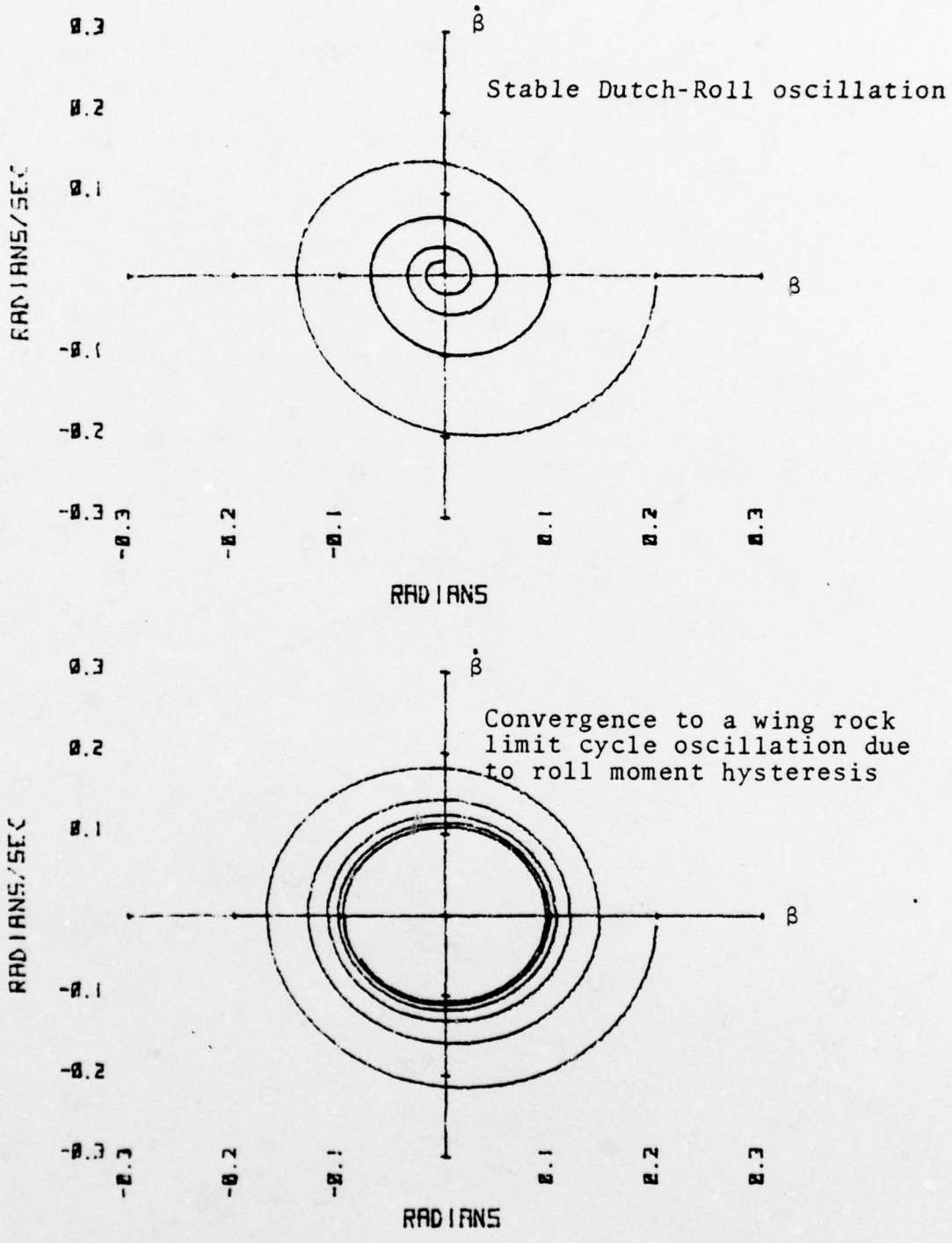

Figure 6. Phase Plane Plots of Dutch-Roll and Roll Hysteresis Induced Wing Rock Limit Cycle.

($\Delta L = 1$) via the relay action mechanism. The relay action was simulated on the analog computer by patching the output of sideslip velocity through a comparator and relay module whose output of $\pm$ 10 volts was a function of the sign of $\dot{\beta}$. The same mechanism was simulated on the digital computer by making use of the predefined function, SGN, which returns a plus or minus 1 value according to the sign of its argument.

Two rather unusual features that require some elaboration are present in the time history plots. Specifically, the unusual shape of the roll rate curve with roll hysteresis applied was believed due to the sudden application of a rolling moment step input via the relay action. The lower of the two peaks per half cycle was judged the more accurate for analysis (refer figure 4). Secondly, a solution was obtained to equation (08) using a negative value of the roll hysteresis, which except for a change in sign was identical to the solution obtained using a positive value of equal magnitude roll hysteresis (Table I). However, both the analog and digital computers gave a time history response for the same value of hysteresis that was heavily damped or essentially deadbeat after one cycle. The numerical prediction was therefore assumed to be in error, although this did not reflect on the validity of the mathematical modeling used. Rather, it was concluded that the predicted solution failed to account for the overall interaction of the production aircraft's stability derivatives during a dynamic propagation of the motion. Stated another way, the hysteresis action would only traverse

in the counter-clockwise direction about the loop in figure 2. A similar check was made on yaw hysteresis with identical results.

Figure 7 shows the limit cycle caused by applying yaw hysteresis via the same relay mechanism used for roll hysteresis. When compared to the corresponding time history plot for the Dutch-Roll oscillation in figures 4 and 5, the motion induced by yaw hysteresis in figure 7 bears a remarkable resemblance. The phase angle relationship and period (Table I) are identical to the Dutch-Roll. From this, one may conclude that yaw hysteresis is essentially a forced Dutch-Roll response.

The combination of roll and yaw hysteresis reflects to some extent the relative influence of each on the total aircraft response. As one might intuitively expect, the resulting motion was a compromise or average of the individual effects of roll and yaw hysteresis as previously seen. In Table I it was pointed out that the maximum value for roll rate was not necessarily achieved when sideslip velocity, $\dot{\beta}$, was zero. This was confirmed by the plot in figure 9. (Although not explicitly shown in figure 9, $\dot{\beta}$ was obviously zero when β was an extremum). There were many more combinations of roll and yaw hysteresis that could have been tried; however, this was not considered feasible nor productive. Again, the relay action can be seen in the behavior of the roll rate response in figure 9. The distortion of the roll rate response curve was due to the combined effects of roll and yaw hysteresis. Likewise, the phase shift for bank angle is a compromise between that seen in figures 7 and 5.

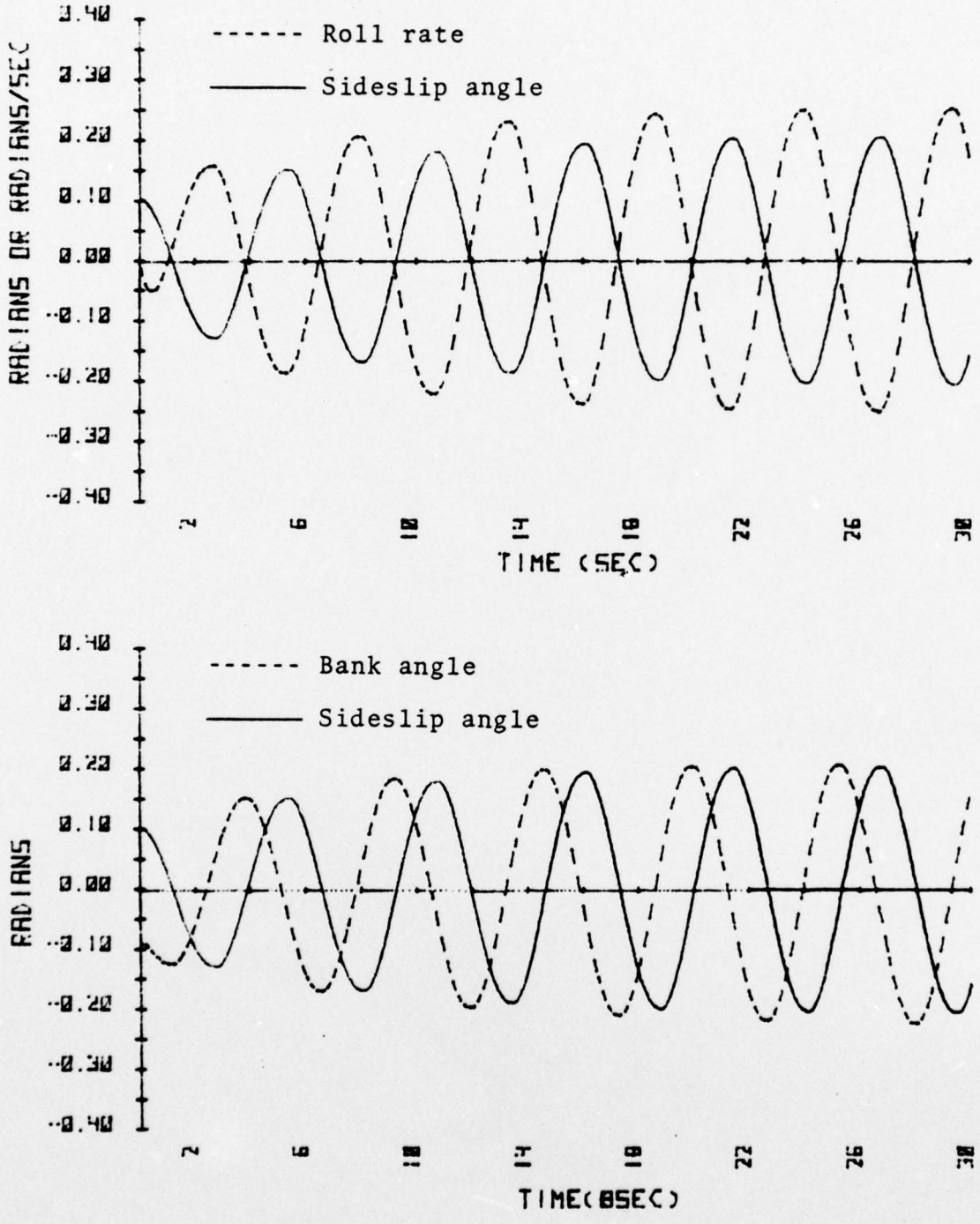

Figure 7. Time History of Divergence to Wing Rock Limit Cycle Due to Yaw Hysteresis.

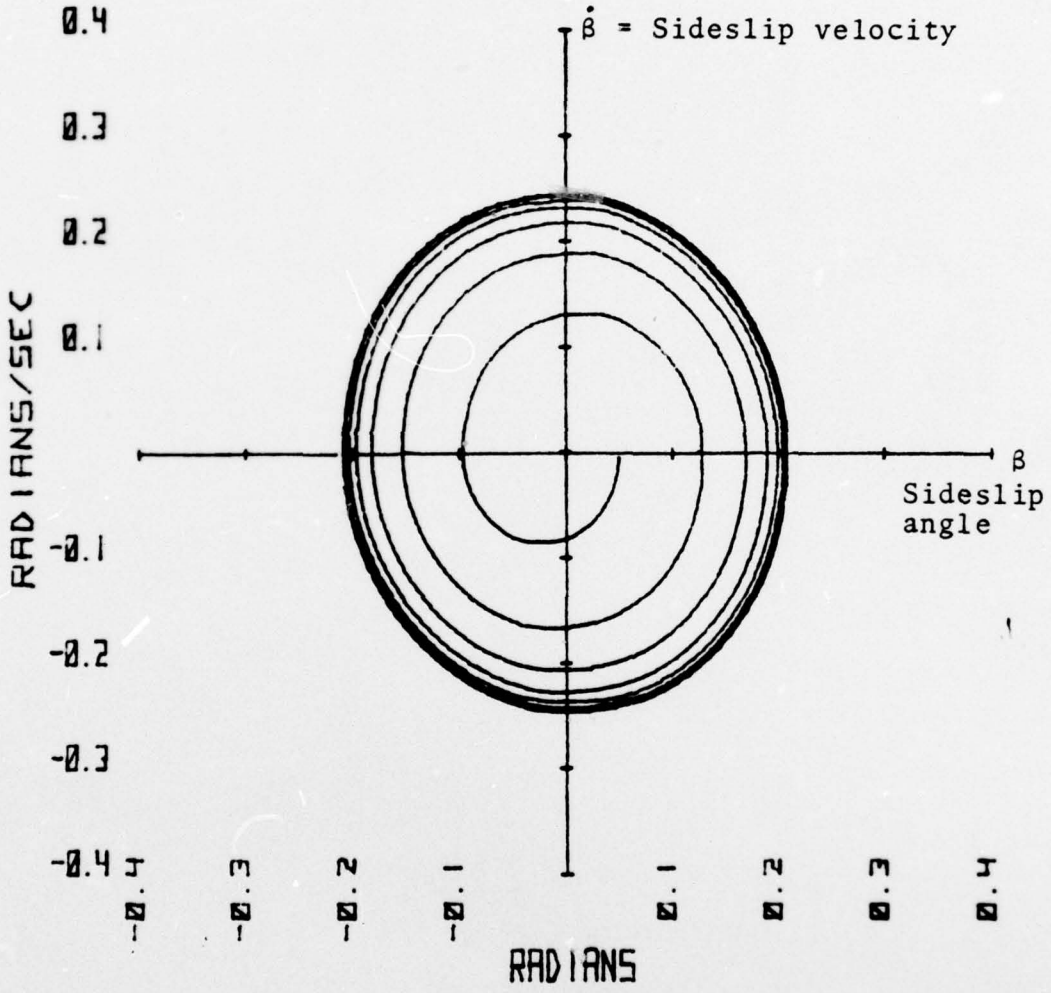

Figure 8. Phase Plane Plot of Divergence to Yaw Hysteresis Induced Wing Rock Limit Cycle.

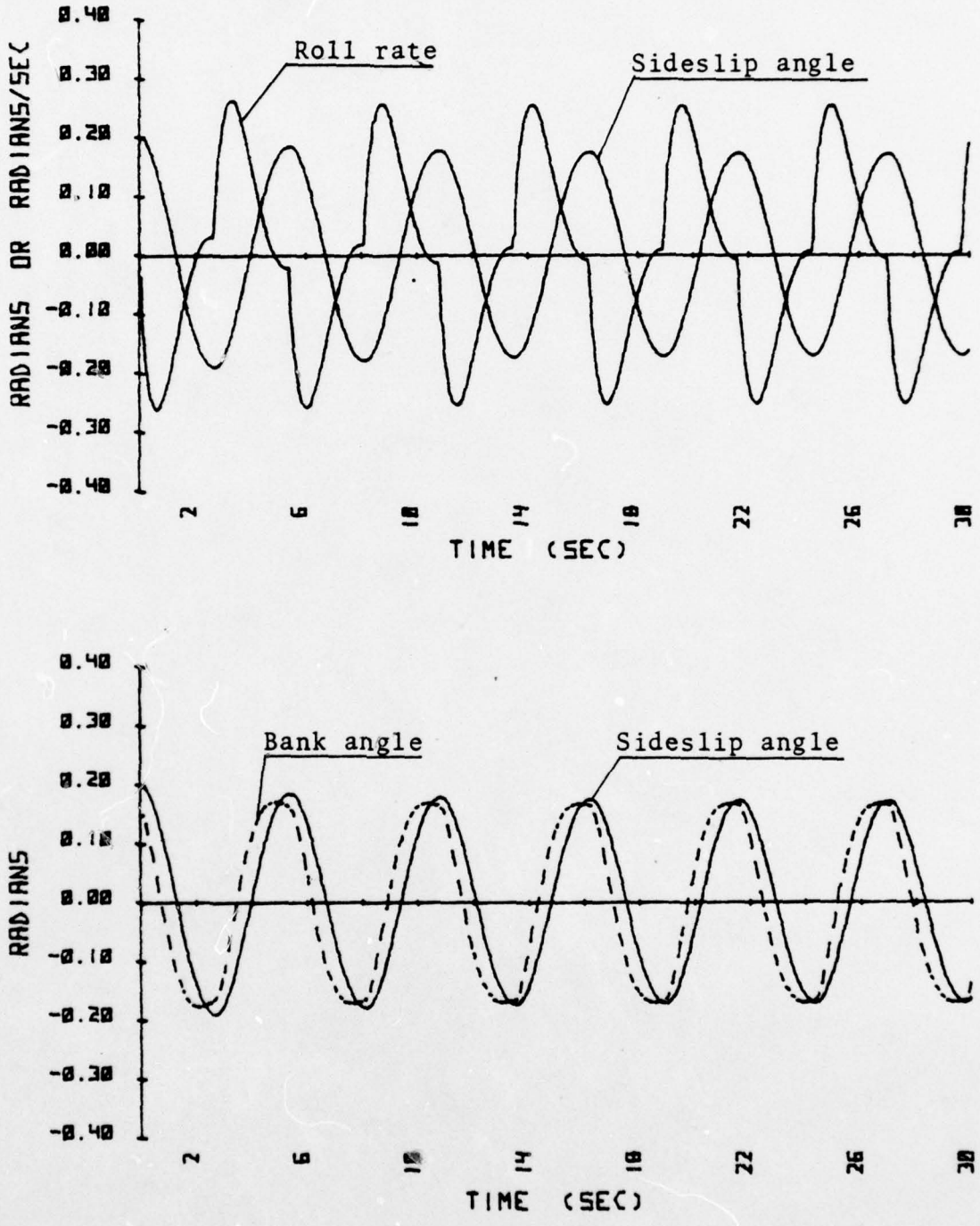

Figure 9. Wing Rock Limit Cycle Due to Combined Roll and Yaw Hysteresis.

With the exception of figures 6 and 8, the limit cycle oscillations were not completely developed at the termination of the time allotted for the numerical integration. This was due primarily to the limited plotting space available, whereas in figures 6 and 8 the phase plane plot was not so restricted, and clearly shows convergence or divergence to the limit cycle amplitudes after release from the initial conditions.

For the sake of visualization, one could equate the values of roll or yaw hysteresis to a deflection of the appropriate control surface, i.e., a nominal $\pm$ 10% of available control power from the aileron or rudder control surfaces. From the analysis conducted on the analog computer, with its real time ability to reflect changes in the problem variables, it became apparent after some experimentation that the cross coupling between roll rate and yawing moment through the adverse yaw stability derivative, N_p, though weak, was responsible for excitation of the limit cycle when roll hysteresis was applied. Yaw hysteresis, on the other hand, acted directly through the directional stability derivative, N_β, to produce a yawing moment.

3. Summary of Hysteresis Induced Wing Rock

There are several significant points worth considering from this analysis and the data presented in Table I and figures 3-9. These include:

(1) The amplitudes of the limit cycle were directly dependent upon the magnitude of applied hysteresis.

(2) The period of the limit cycle was independent of the magnitude of applied hysteresis.

(3) While the roll rate was 180 degrees out of phase with the sideslip angle for the Dutch-Roll oscillation, it was exactly in phase for the limit cycle due to roll hysteresis.

(4) In addition to phase differences, the ratio of bank angle to sideslip angle was three times greater for the limit cycle due to roll hysteresis than for the Dutch-Roll oscillation.

(5) The limit cycle for yaw hysteresis is essentially a forced Dutch-Roll response. Frequency and phase angle relationships are unchanged from the Dutch-Roll.

(6) Reversing the relay action dependence on the sign of $\dot{\beta}$ results in a deadbeat response. Therefore, a wing rock limit cycle is dependent upon the sign of roll or yaw hysteresis.

(7) Combined yaw and roll hysteresis produces a limit cycle response which is essentially a compromise or average of the two effects.

C. ANOTHER FORM OF AERODYNAMIC NONLINEARITY

1. Previous Research

As stated earlier, some research has been done and reported by Ross [Ref. 3] on wing rock as a limit cycle caused by nonlinear aerodynamics interacting with an unstable Dutch-Roll oscillation. Ross reports that a wing rock limit cycle occurred on the Handley Page 115 testbed aircraft as the result of increasing the angle of attack to a critical point where any small lateral-directional perturbation excited an alternating wing rock motion, which steadily grew to a constant amplitude with the controls fixed. The motion would immediately damp to zero when the pilot commanded a reduction in the angle of attack below critical. The Handley Page 115 is a British aircraft designed to serve as a flying testbed primarily for research on the Supersonic Transport and has

geometric characteristics similar to many current tactical aircraft, i.e., thin swept delta wings and a slender fuselage.

In modeling the motion observed in flight and wind-tunnel tests, Ross essentially took the linearized equations describing lateral-directional motion and imposed a nonlinearity on yawing moment due to sideslip, N_β. The extent of the nonlinearity was reflected in a polynomial of degree sufficient to match flight and wind-tunnel data which indicated a nonlinear variation of aerodynamic moments and forces as a function of sideslip angle. A fifth order polynomial (in odd powers only) was proposed initially; however, as Ross pointed out, a cubic nonlinearity was sufficient to yield good agreement with experimental results of wing rock. Ross concedes that although nonlinearities existed in the dihedral effect and sideforce characteristic, these were considered relatively insignificant and thus ignored.

An analysis follows which resulted from an intention to simplify the mathematical modeling proposed by Ross and provide a better analytical tool for use in analyzing lateral-directional motion at angles of attack near stall. As the reader will see, the analysis and conclusions presented here do not necessarily agree with those of Ref. [3].

2. Theory

As a means of simplification, the sideforce equation and the accompanying spiral divergence mode were, as in the hysteresis evaluation, assumed to be insignificant and thus eliminated from the equation set describing lateral-directional motion. This is not unreasonable, as flight tests involving

aircraft exhibiting wing rock have shown that the sideforce is sufficiently small as to be non-discernible to the pilot and has virtually no effect on the heading or ground track. Therefore, the equations of motion applicable to this analysis are the same as in the section on hysteresis, i.e., equations

$$\ddot{\beta} = -N_\beta \beta + N_r \dot{\beta} - N_p p \qquad (03a)$$

$$\dot{p} = L_\beta \beta - L_r \dot{\beta} - L_p p \qquad (03b)$$

Ross concluded that the term which contributed most to the limit cycle in view of an unstable Dutch-Roll oscillation was a cubic nonlinearity in yawing moment due to sideslip. For this analysis the cubic nonlinearity was introduced as:

Yawing moment due to sideslip = $N_\beta \beta = N_\beta (1 + \epsilon \beta^2) \beta$

where ϵ is a scalar of arbitrary magnitude which facilitated varying the desired level of nonlinearity for a given analysis. It was necessary to reduce the set of simultaneous differential equations in (03) to a single third order equation as a function of a single independent variable, β. From equation (03a) the cubic nonlinearity yields:

$$\ddot{\beta} = -N_\beta \beta (1 + \epsilon \beta^2) + N_r \dot{\beta} - N_p p \qquad (03c)$$

Taking the derivative of this equation with respect to time yields:

$$\dddot{\beta} = -N_\beta \dot{\beta} - 3\epsilon N_\beta \beta^2 \dot{\beta} + N_r \ddot{\beta} - N_p \dot{p}$$

(12)

Solving for $\dot{\rho}$ in (12) as a precursor to elimination of the variable ρ from the equations set yields:

$$\dot{\rho} = \frac{1}{N_\rho}\left[-\ddot{\beta} - N_\beta(1+3\epsilon\beta^2)\dot{\beta} + N_r\ddot{\beta}\right] \tag{13}$$

Now solve for ρ from equation (03a) and substitute the result in equation (03b).

$$\dot{\rho} = L_\beta\beta - L_r\dot{\beta} + L_\rho\rho$$

$$\dot{\rho} = L_\beta\beta - L_r\dot{\beta} + \frac{L_\rho}{N_\rho}\left[-\ddot{\beta} - N_\beta(1+\epsilon\beta^2)\beta + N_r\dot{\beta}\right] \tag{14}$$

Equations (13) and (14) can now be equated to complete the elimination of ρ and yield a single third order differential equation in the single variable β, from which the analysis proceeds.

$$\frac{1}{N_\rho}\left[-\dddot{\beta} - N_\beta(1+3\epsilon\beta^2)\dot{\beta} + N_r\ddot{\beta}\right] = L_\beta\beta - L_r\dot{\beta} + \frac{L_\rho}{N_\rho}\left[-\ddot{\beta} - N_\beta(1+\epsilon\beta^2)\beta + N_r\dot{\beta}\right]$$

Clearing through by a minus N_ρ and collecting terms yields:

$$\dddot{\beta} - (N_r + L_\rho)\ddot{\beta} + \left[N_\beta(1+3\epsilon\beta^2) - N_\rho L_r + N_r L_\rho\right]\dot{\beta} + \left[N_\rho L_\beta - L_\rho N_\beta(1+\epsilon\beta^2)\right]\beta = 0$$

It is convenient to introduce the following notation for ease of writing:

$$A = -(N_r + L_p)$$

$$B = b_1\beta + b_3\beta^3$$

$$C = c_1\beta + c_3\beta^3$$

where:

$$b_1 = N_\beta + N_r L_p - N_p L_r$$

$$b_3 = \epsilon N_\beta$$

$$c_1 = N_p L_\beta - L_p N_\beta$$

$$c_3 = -\epsilon N_\beta L_p$$

Thus, the resulting third order equation can be expressed in a more general form as:

$$\frac{d^3\beta}{dt} + A\frac{d^2\beta}{dt^2} + \frac{dB(\beta)}{dt} + C(\beta) = 0 \tag{15}$$

This is a nonlinear differential equation for which there is no analytical solution. Necessary assumptions were made in order to gain an approximate solution as discussed in the following.

3. Analysis

With the resulting general form of the equation of motion given by (15) it was possible to proceed with an analysis of the motion similar to that presented by Ross, differing only in the degree of simplicity. Recall that the simplicity was gained by making the assumption that $\psi = -\beta$ or that the aircraft remains on a steady track (without heading deviation) while engaged in wing rock. Ross, however, did not make this assumption but rather included the side force equation resulting in a fourth order system. It was further assumed, as did Ross, that the oscillatory motion regardless of damping could be represented by the following:

$$\beta = De^{\lambda t}\cos\omega t = \sigma\cos\theta$$

$$\text{where} \quad \left.\begin{aligned} \sigma &= De^{\lambda t} \\ \theta &= \omega t \end{aligned}\right\} \Longrightarrow \begin{aligned} \lambda &= \dot{\sigma}/\sigma \quad \text{or} \quad \dot{\sigma} = \lambda\sigma \\ \omega &= \dot{\theta} \end{aligned} \qquad (16)$$

This simply says that wing rock motion can be described as a sinusoidal oscillation with sideslip amplitude considered as a slowly varying function of damping and time. The shorthand notation of sigma (σ) and ~~theta~~ (θ) was used for writing convenience.

In order to gain an approximate solution to equation (15), the Krylof and Bogoliubof (KB) method, Ref. [7] was used.

This method has been used extensively to analyze second order systems with "weak" nonlinearities. With the exception of this analysis, as well as that done by Ross on the fourth order system, no other reference to use on higher than second order systems could be found. Nevertheless, there was no apparent mathematical restriction to applying the KB method to the third order system of equation (15). Moreover, the KB method is applicable given the assumption that the amplitudes of a vibratory system vary only slightly over a single cycle. Thus, the terminology often used is the assumption of slowly varying parameters, which is equally valid when considering a slowly divergent Dutch-Roll oscillation.

It was necessary to take the assumed form of the solution in equation (16) for the dependent variable, β, and derive the first, second and third derivatives, which were:

$$\frac{d\beta}{dt} = \sigma\,[\lambda \cos\theta - \omega \sin\theta] \tag{17a}$$

$$\frac{d^2\beta}{dt^2} = \sigma\,[(\lambda^2-\omega^2)\cos\theta - 2\omega\lambda \sin\theta] \tag{17b}$$

$$\frac{d^3\beta}{dt^3} = \sigma\,[(\lambda^3-3\omega^2\lambda)\cos\theta + (\omega^3-3\omega\lambda^2)\sin\theta] \tag{17c}$$

Substituting equations (17) into equation (15) yields:

$$\frac{d^3\beta}{dt^3} = -A\frac{d^2\beta}{dt} - \frac{dB(\beta)}{dt} - C(\beta)$$

$$= \sigma\{-A[(\lambda-\omega^2)\cos\theta - 2\omega\lambda\sin\theta] - b_1[\lambda\cos\theta - \omega\sin\theta]$$

$$-3b_3[\lambda\cos\theta - \omega\sin\theta]\sigma^2\cos^2\theta - C_1\cos\theta - C_3\sigma^2\cos^3\theta\}$$

$$\therefore \frac{d^3\beta}{dt^3} = \sigma\{-[A(\lambda^2-\omega^2)+b_1\lambda+C_1]\cos\theta + [2A\omega\lambda + b_1\omega]\sin\theta$$

$$-[3b_3\lambda + C_3]\sigma^2\cos^3\theta + 3b_3\omega\sigma^2\sin\theta\cos^2\theta\} \tag{18}$$

Equation (18) is of the form:

$$\frac{d^3\beta}{d\tau} = \tau F(\lambda, \omega, \tau, \cos\theta, \sin\theta)$$

The governing principle of the KB method says that since the amplitudes are considered essentially constant over a given cycle (slowly varying parameters), then the average value over the cycle is a sufficiently close approximation to the actual maximum value. This averaging process, when applied to equation (18), yields the following:

$$[\lambda^3 - 3\omega^2\lambda] = \frac{1}{\pi}\int_0^{2\pi} F\cos\theta\, d\theta$$

$$[\omega^3 - 3\omega\lambda^2] = \frac{1}{\pi}\int_0^{2\pi} F\sin\theta\, d\theta$$

$$[\lambda^3 - 3\omega^2\lambda] = \frac{1}{\pi}\left\{-\pi\left[A(\lambda^2 - \omega^2) + b_1\lambda + c_1\right] - \frac{3}{4}\pi\left[3b_3\lambda + c_3\right]\tau^2\right. \quad (19a)$$

$$[\omega^3 - 3\omega\lambda^2] = \frac{1}{\pi}\left\{\pi\left[2A\omega\lambda + b_1\omega\right] + \frac{3}{4}\pi b_3\omega\tau^2\right\} \quad (19b)$$

Arriving at equations (19) necessarily involved the orthogonality principles of integration as shown below:

$$\int_0^{2\pi}\cos^2\theta\, d\theta = \int_0^{2\pi}\sin^2\theta\, d\theta = \pi$$

$$\int_0^{2\pi}\cos^4 d\theta = \frac{3}{4}\pi\int_0^{2\pi}\sin\theta\cos\theta\, d\theta = 0$$

$$\int_0^{2\pi}\sin\theta\cos^3\theta\, d\theta = 0 \quad \text{AND} \quad \int_0^{2\pi}\sin^2\theta\cos^2\theta\, d\theta = \frac{\pi}{4}$$

Note that equations (19) yield the characteristic equation for the stable system, when the nonlinearities vanish which are contained in the odd subscripted variables, b_3 and c_3:

$$(\lambda + i\omega)^3 = [\lambda^3 - 3\omega^2\lambda] - i[\omega^3 - 3\omega\lambda^2]$$

Thus $$(\lambda + i\omega)^3 = -A(\lambda + i\omega)^2 - b_1(\lambda + i\omega) - c_1$$

which is equivalent to:

$$s^3 + As^2 + b_1 s + C_1 = 0$$

Assuming that a limit cycle occurs, the following conditions must hold:

$$\beta_s = \sigma_s \cos \theta$$

$$\sigma_s = D e^{\lambda t}$$

Thus $\lambda_s = 0$ = damping

$\sigma_s = D$ = constant

where the subscript, s, is used to denote steady-state conditions. Hence, from equations (19), with the limit cycle conditions of zero damping imposed, $\lambda_s = 0$, there is

$$0 = A\omega_s^2 - C_1 - 3/4\, C_3 \sigma_s^2$$

$$\omega_s^3 = b_1 \omega_s + 3/4\, b_3 \omega \sigma_s^2$$

It can be reasonably assumed that a limit cycle will not occur for a frequency $\omega = 0$. The phrase "reasonably assumed" is used advisedly. Although it seems intuitive that such an assumption would be valid, some researchers, notably Parkinson [Ref. 8] detailed a study of the transverse galloping of a long prism of square section in a steady flow field in which the subject body possessed an unstable focus at rest. Whether this means that $\omega = 0$ is a valid solution for a wing rock limit cycle, and thus cannot be discarded, remains largely unanswered. Nevertheless, such an assumption was made, as did Ross, enabling elimination of the ω_s term between the two above equations yielding the final equations describing the limit cycle.

$$A(b_1 + \tfrac{3}{4} b_3 \sigma_s^2) - C_1 - \tfrac{3}{4} C_3 \sigma_s^2 = 0$$

$$\tfrac{3}{4}(b_3 - C_3)\sigma_s^2 + Ab_1 - C_1 = 0$$

$$\sigma_s^2 = -\frac{4}{3}\left(\frac{Ab_1 - C_1}{b_3 - C_3}\right) = \frac{4}{3}\left(\frac{Ab_1 - C_1}{C_3 - b_3}\right)$$

$$\sigma_s = 1.1547 \left(\frac{Ab_1 - C_1}{C_3 - b_3}\right)^{1/2} \qquad (20)$$

The frequency, ω_s, for the limit cycle can then be obtained as:

$$\omega_s = \left\{b_1 + b_3\left(\frac{Ab_1 - C_1}{C_3 - b_3}\right)\right\}^{1/2} \qquad (21)$$

Recall that one of the preconditions for the limit cycle as proposed by Ross was that the aircraft must possess an unstable Dutch-Roll mode of slowly varying parameters, which is constrained in amplitude by a positive cubic nonlinearity in yawing moment (yawing moment increasing with sideslip angle). Yet there was nothing explicitly incorporated into the mathematical model, which yielded equations (20) and (21), that would account for this condition. Instead, it was assumed that a limit cycle existed due to a constrained motion instability. The modeling proceeded on this basis with the motion constraint explicitly incorporated by $N_\beta(1 + \epsilon\beta^2)\beta$. This should not be interpreted to mean that a limit cycle will occur only if there is a divergence of the vibrating system initially (refer to section III.A); however, when applied to aircraft dynamics this is probably the most common way limit cycle oscillations occur, as was experienced by Ross and has been experienced by the author as well.

The effect of inducing a limit cycle via a positive nonlinearity on N_β at high angle of attack is intuitively appealing. This would amount to increasing directional stability with sideslip, or the spring in the spring mass damper gets stiffer with displacement from equilibrium, until there is an equilibrium established between the energy contained in the unstable Dutch-Roll and that absorbed by the spring. Physically, this could correspond to an aircraft exhibiting a decrease in directional stability at low sideslip angles and high angle of attack due to a turbulent, low energy flow field emanating from the wing and engulfing ehe empennage section, thus reducing the restoring moments generated by stabilizing and/or control surfaces. This is often the case for the tactical high performance aircraft. However, as the tail is yawed out of the low energy flow and into a lower-turbulence-level, higher energy flow (higher kinetic energy or dynamic pressure), the directional stability will increase. Thus, the premise of an unstable motion constrained by a nonlinearity in directional stability would appear to be valid.

The F-94 airplane as originally used had a stable Dutch-Roll; therefore, it was necessary to destabilize the airplane artificially for the sake of conducting wing rock studies. The primary means of achieving an unstable Dutch-Roll oscillation consisted of altering the sign and magnitude of the yaw rate damping derivative, N_r. The effect of this can be seen in figure 10, where the motion slowly diverges at a frequency equal to the stable Dutch-Roll. Since the

denominator of equation (20) is positive, and in order to ensure that the radical term remained positive, it was necessary to alter a second derivative such that $Ab_1 > c_1$. After some manipulation, the following derivatives were changed as indicated:

$$N_r = .02$$

$$N_p = -.3$$

a. Predictions Based on Analytical Solution

The following is a sample calculation of a predicted limit cycle using equations (20) and (21).

$$A = -(N_r + L_p) = 2.4357$$

$$b_1 = N_\beta + N_r L_p - N_p L_r = 1.7274$$

$$c_1 = N_p L_\beta - N_\beta L_p = 4.0916$$

$$b_3 = \epsilon N_\beta = 1.3214\epsilon$$

$$c_3 = -\epsilon N_\beta L_p = 3.245$$

$$\sigma_s = 1.1547\left(\frac{(2.4357)(1.7274) - 4.0916}{-\epsilon(1 - 2.4557)(1.3214)}\right)^{1/2}$$

with $\epsilon = 5$

$$\sigma_s = .1267 \text{ Rad} = 7.15 \text{ Deg}$$

$$\omega_s = 1.3454 \text{ Rad/sec}$$

$$T_s = 4.67 \text{ sec.}$$

In addition to the analog and digital computer programs previously mentioned, programs were likewise written and executed based upon the reduced third order equation (15).

These are presented in Appendix D and F. These programs were used primarily to compare with the results based on the two equation system (equations 03b, 03c) to ensure consistency and accuracy to the maximum extent possible of the mathematical modeling that led to equations (20) and (21). The same plotting program of Appendix C was used. Heavy reliance was placed upon the analog computer for qualitative analysis, where changes could be made and their effects observed immediately.

b. Verification of Predictions

The limit cycle predicted by the above sample calculation was not obtained. Rather, another limit cycle of lower steady state sideslip amplitude, figure 10, occurred almost immediately upon release from initial conditions with a level of nonlinearity, $\epsilon = 5$.

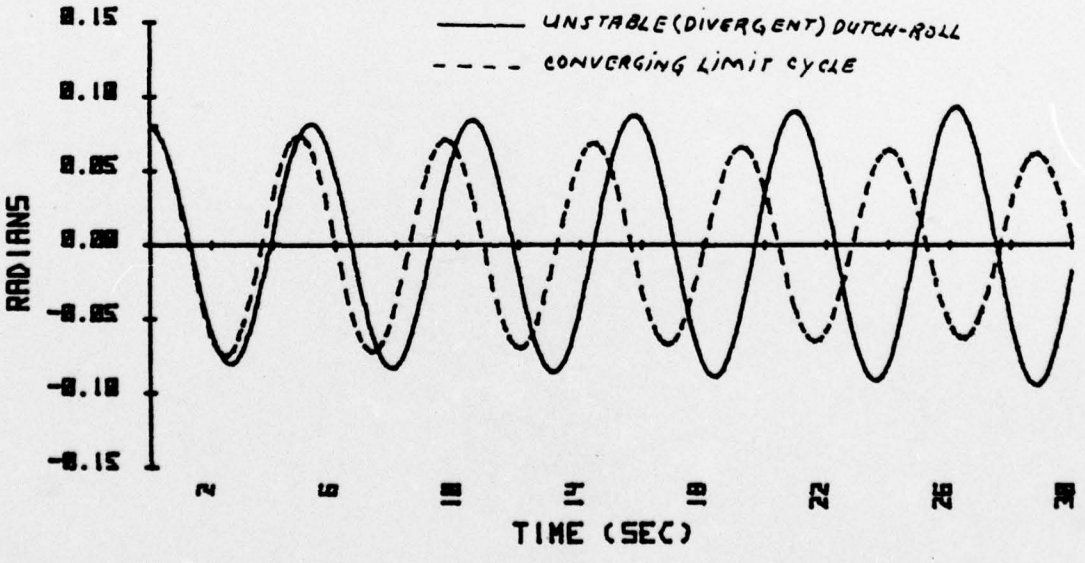

Figure 10. Time History of Wing Rock Limit Cycle and Divergent Dutch-Roll.

The value of the predicted σ_s = .13 radians was greater than the initial condition β_o = .08. Thus, according to theory and the fact that an unstable Dutch-Roll existed as shown in Fig. 10, the motion should have slowly diverged to the predicted steady state values. Similarly, an initial condition greater than the predicted value of σ_s was tried (not shown) to see if the motion would converge to the limit cycle; however, the time history was essentially identical to the first in that a limit cycle again developed with an amplitude very nearly the same as the initial conditions. Therefore, the wing rock limit cycle appeared to be a function of the stability derivatives, N_r and N_p, and the initial conditions, rather than of the value of the nonlinearity in yawing moment.

The effect of the level of nonlinearity as viewed on the analog computer was merely to alter the frequency, with no change in amplitude. On the other hand, the predicted frequency, ω_s, agreed very well with experimental data. For the above sample, the predicted ω_s in terms of the period (where period $T_s = \frac{2\pi}{\omega_s}$) was 4.67 sec, while experimental results showed 4.7 sec. This close agreement on frequency held for changes in the level of nonlinearity ϵ, as well as changes in the stability derivatives, as long as the requirement $Ab_1 > c_1$ was satisfied, as previously discussed.

Experimentation on the analog computer showed that the time history response behaved as if neutral stability existed. When considering motion without nonlinearity imposed, the Routh Stability Criterion can be used to determine the

neutral stability boundary, and it appeared at first that possibly the Routh discriminant had been inadvertently satisfied through the manipulation of N_r and N_p; i.e., $Ab_1 - c_1 = 0$, is directly proportional to Routh discriminant. However, this was not the case as $Ab_1 - c_1$ was found equal to 0.1158.

4. Summary of Wing Rock Induced by Nonlinear Yawing Moment

Now, an obvious question arises as to the source of disagreement between these findings and those of Ross. The main difference with this analysis and that carried out by Ross was the simplification imposed at the beginning, i.e., that the sideforce equation and accompanying spiral mode were insignificant and need not be considered. Since the F-94 possessed no natural instability in the Dutch-Roll at the angle of attack tested, the artificial manipulation of the stability derivatives N_r and N_p, as discussed above, may have been so arbitrary as to not correctly represent the characteristics previously exhibited by the Handley Page 115, and documented by Ross. Whether these or other concepts were the source for the disagreement in results is unknown. Possibly the analysis Ross presented for the Handley Page 115 was peculiar to that aircraft, although intuitively one would tend to argue in favor of the premise that a limit cycle would occur for an unstable Dutch-Roll in the presence of an increasing yawing moment with sideslip angle. In view of this, it is recommended that follow-on research be conducted using the complete set of equations of motion, i.e., including

the sideforce equation and the analysis technique presented here to make a more conclusive determination as to the validity of the concept that a wing rock limit cycle can be the result of an unstable Dutch-Roll coupled with a cubic nonlinearity in N_{β}. Moreover, any additional research should be conducted on an aircraft known to exhibit wing rock motion such as the Handley Page 115 or preferably on an operational, tactical aircraft such as the Northrop T-38 or F-5.

IV. CONCLUSIONS AND RECOMMENDATIONS

The existence of a lateral-directional aircraft limit-cycle oscillation, due to an aerodynamic hysteresis corresponding to a roll or yaw moment relay action that is dependent upon the sign of sideslip velocity, has been demonstrated. The use of state variable notation allowed the limit-cycle motion to be expressed in a concise and clear manner.

Although bank angle was not a state variable in the analysis and hence could only be estimated from roll rate, the inclusion of this term by the introduction of a sideforce equilibrium equation is practicable for a more detailed analysis. However, in keeping with the purpose of the analyses presented here, to illustrate a concept, the only equations used were those absolutely required to achieve that goal.

The existence of a wing rock limit cycle oscillation due to a nonlinear yawing moment, as reported by Ross [Ref. 3], was not confirmed by the analysis presented here. The essence of the differences in the two analyses was in the basic assumption that the sideforce equilibrium equation need not be included. Such an assumption is based in large part upon personal flight test experience of the author, in which the characteristics of wing rock at high angle of attack have clearly indicated that yaw excursions are relatively small, thus adding support to the contention that sideforces be assumed negligible.

From the exhaustive experimental observations made in the laboratory, albeit using an aircraft that was known not to possess any wing rock limit cycle characteristics, serious doubts have been raised concerning the generality of Ross' analysis. While on the one hand the concept of a nonlinear spring, as applied to aircraft dynamics, and the "limiting" of the divergent Dutch-Roll oscillation, has intuitive appeal, experimental results using analog or digital modeling consistently indicated an effect only on the frequency of the vibration, with no effect on damping. Indeed, a limit cycle was achieved based upon the modeling criteria used by Ross, but not as predicted with respect to steady state amplitude. However, the predicted and resulting experimental value for frequency of the oscillation showed excellent agreement. Of the limit cycle obtained, the damping appeared to be a function of the modified stability derivatives necessary to artificially destabilize the Dutch-Roll of an otherwise stable test aircraft (F-94) rather than of the level of the cubic nonlinearity.

The source of disagreement between the results obtained here and those of Ross remained unknown at the termination of this research. Sufficient time was unavailable to pursue the question further; however, it is recommended that follow-on research be conducted, when time permits, to make a more detailed analysis, possibly including the sideforce equation, in an effort to determine the source of disagreement between the two analyses, which has led to quite different aircraft responses.

Finally, it is hoped that these analyses will make clearer that interpreting an actual aircraft time history as representing a Dutch-Roll mode with exactly zero damping may be misleading, since a motion with very similar appearance could be a limit cycle due to aerodynamic relay, or hysteresis actions, or nonlinear yawing and rolling moments as posed by Ross. The direct problem of determining the time response of an aircraft due to forcing functions, be they linear or nonlinear, is tractable. The inverse problem of identifying the plant from the aircraft time histories (known as aircraft parameter identification) is much more difficult, because of the uncertainties in estimating types of plant nonlinearities.

```
10 REM: PROGRAM TO SOLVE FOR PERIOD OF AIRCRAFT LAT-DIR LIMIT CYCLE OSCILLATION
20 REM: AND MAXIMUM VALUES OF STATE VARIABLES  RESULTING FROM RESPONSE TO STEP
25 REM: INPUT. MAKES USE OF DATA SUPPLIED FROM THE BASMAT PROGRAM; I.E.,
26 REM: THE STATE TRANSITION MATRIX.  USES SOLUTION FOR STEP INPUT GIVEN
27 REM: ON PAGE 709 OF OGATA
30 DIM A[3,3],B[3,3],C[3,3],D[3,3],W[3,1],I[3,3]
31 DIM F[3,3],E[3,3],G[3,3],H[3,3],X[3,1]
32 REM: A MATRIX IS ORIGINAL PLANT. B,C,D ARE STATE TRANS. MATRIXES. W MATRIX
33 REM: STORES EIGENVALUES
40 MAT READ A,B,C,D,W
50 MAT PRINT A,B,C,D,W
60 MAT A=INV(A)
65 REM: INPUT EIGENVALUES FROM BASMAT. REAL VALUE FOLL BY ABS VALUE OF IMAGINARY
70 DISP "EIGENVALUES FROM BASMAT";
80 INPUT L1,L2,L3
90 T1=T2=0
91 MAT I=IDN
100 DISP "GUESS FOR PERIOD";
110 INPUT T
120 T=T/2
125 REM: BEGIN ITERATIVE ROUTINE
130 FOR I=1 TO 3
140 FOR J=1 TO 3
150 F[J,I]=B[J,I]*EXP(L1*T)+(C[J,I]*COS(L3*T)+D[J,I]*SIN(L3*T))*EXP(L2*T)
160 NEXT J
170 NEXT I
175 REM: MATRIX ALGEGRA
180 MAT E=I+F
190 MAT E=INV(E)
200 MAT G=E*A
210 MAT H=F-I
220 MAT E=G*H
230 MAT X=E*W
235 REM: ESTABLISHING PLUS AND MINUS VALUES OF FUNCTION FOR INTERVAL HALVING
240 IF T1#0 AND T2#0 THEN 320
250 IF X[2,1]>0 THEN 290
260 T1=T
265 REM: PROGRAM LISTING CONTINUED ON NEXT PAGE
```

```
266 REM: CONTINUED FROM PREVIOUS PAGE
270 PRINT X[2,1]
275 REM: IF TWO VALUES OF OPPOSITIE SIGN NOT FOUND RETURN FOR ANOTHER GUESSED
276 REM: INPUT FROM KEYBOARD
280 GOTO 100
290 T2=T
295 IF T1#0 THEN 320
300 PRINT X[2,1]
310 GOTO 100
315 REM: INTERVAL HAVING ROUTINE
320 IF ABS(X[2,1])>1E-04 THEN 360
330 PRINT "T="2*T;"BETA="X[1,1];"BDOT="X[2,1];"RR="X[3,1]
340 PRINT
350 STOP
360 IF X[2,1]<0 THEN 385
365 T2=T
370 T=(T-T1)/2+T1
380 GOTO 130
385 T1=T
390 T=(T2-T)/2+T
400 GOTO 130
405 REM: DATA STATEMENTS CAN START HERE CONTAINING VALUES FROM STATE TRANSITION
500 REM: ENTERED CONTIGUOUSLY BY ROWS BEGINNING WITH TOP MATRIX FROM BASMAT P.O.
550 REM
599 REM
600 REM: END OF THIS PROGRAM LISTING
```

```
1 REM: PROGRAM TO NUMERICALLY INTEGRATE A SYSTEM OF 3 FIRST ORDER ORDINARY
2 REM: DIFFERENTIAL EQUATIONS.  INCLUDES CAPABLITY TO SPECIFY YAW/ROLL
3 REM: HYSERESIS AND/OR CUBIC NONLINEARITY IN YAWING MOMENT.  SYSTEM HAS BEEN
4 REM: REDUCED TO TWO EQUATIONS WITH ONE SECOND AND ONE FIRST ORDER EQUATION.
5 REM: EQUATIONS INTEGRATED REPRESENT LAT-DIR EQUATION OF MOTION LESS SIDEFORCE
6 REM: EQULIBRIUM EQUATIONS; I.E, DUTCH-ROLL AND ROLL MODES.  USES EULER
7 REM: PREDICTOR-CORRECTOR METHOD WITH ITERATION ON CORRECTIONS.
10 DIM A$[30,30],B$[30,30],C$[30,30],D$[30,30]
15 REM: INPUT INITIAL CONDITIONS FOR LAT-DIR MOTION
40 DISP "BETA,BDOT,ROLL RATE,BANK ANGLE";
50 INPUT B0,B1,P0,F
60 DISP "INTEG PERIOD AND STEP SIZE";
70 INPUT L,H
100 DISP "NONLINEAR COEFF.";
110 INPUT E
120 DISP "VALUE FOR NR";
130 INPUT N
132 DISP "YAW MOMENT HYSTERESIS";
134 INPUT N
135 DISP "ROLL MOMENT HYSTERESIS";
136 INPUT L
140 T=0
145 REM: INTEGRATION BEGINS
150 FOR I=1 TO 30
160 FOR J=1 TO 30
170 T=T+H
180 IF T>L THEN 380
190 U1=B0
200 U2=B1
210 U5=P0
215 U6=F
220 GOSUB 390
230 U3=B2
240 U4=P1
246 REM: CONTINUED ON NEXT PAGE
```

```
247 REM: PROGRAM LISTING CONTINUED FROM PREVIOUS PAGE
250 B1=B2*H+B1
260 B0=U2*H+B0
270 P0=P1*H+P0
280 GOSUB 390
281 U7=B2
282 U8=P1
290 B1=((U3+B2)/2)*H+U2
300 B0=((B1+U2)/2)*H+U1
310 P0=((P1+U4)/2)*H+U5
315 F=((P0+U5)/2)*H+U6
316 GOSUB 390
317 IF ABS(U7-B2)>1E-03 OR ABS(U8-P1)>1E-03 THEN 281
318 REM: STORE OUTPUT FOR PLOTTING LATER
320 A[J,I]=B0
330 B[J,I]=B1
340 C[J,I]=P0
350 D[I,J]=F
360 NEXT J
370 NEXT I
375 REM: LINK UP WITH PLOTTING PROGRAM FOR PLOTTING STORED OUTPUT
380 LINK 1
385 REM:  EQUATIONS TO BE INTEGRATED
390 B2=-1.3214*B0*(1+E*B0↑2)+N*B1+0.4*P0
400 P1=-2.822*B0-1.517*B1-2.4557*P0
410 RETURN
415 REM:
416 REM: END OF PROGRAM LISTING
```

```
1 REM: PROGRAM TO PLOT AND LABEL STORED OUTPUT FROM INTEGRATION PROGRAMS
10 DISP "XMIN,XMAX";
20 INPUT X1,X2
30 DISP "YMIN,YMAX";
40 INPUT Y1,Y2
50 SCALE X1-0.2*(X2-X1),X2+0.1,Y1-0.2*(Y2-Y1),Y2+0.1
60 DISP "TIC SPACING XAXIS";
70 INPUT T
80 DISP "TIC SPACING YAXIS";
90 INPUT T1
100 DISP "PHASE PLANE PLOT";
110 INPUT Z
120 IF Z=0 THEN 130
122 XAXIS 0,T,X1,X2
124 YAXIS 0,T1,Y1,Y2
126 GOTO 150
130 XAXIS 0,T,X1,X2
140 YAXIS X1,T1,Y1,Y2
150 LABEL (*,2,1.7,PI/2,6/9)
160 FOR X=X1 TO X2 STEP 2*T
170 IF X=0 AND Z=1 THEN 230
180 IF X#0 THEN 200
190 X=X+T
200 PLOT X,Y1,1
210 CPLOT -4,0
220 LABEL (500)X
230 NEXT X
240 LABEL (*,2,1.7,0,6/9)
245 REM: PROGRAM LISTING CONTINUED ON FOLLOWING PAGE
```

```
246 REM: CONTINUED FROM PREVIOUS PAGE
250 FOR Y=Y1 TO Y2 STEP 2*T1
260 IF Y=0 AND Z=1 THEN 330
270 IF Z=1 THEN 300
280 PLOT X1,Y,1
290 GOTO 310
300 PLOT X1,Y,1
310 CPLOT -7,0
320 LABEL (600)Y
330 NEXT Y
360 T=0
365 PEN
370 FOR I=1 TO 30
380 FOR J=1 TO 30
390 T=T+H
400 IF T>L THEN 440
405 REM: THE FOLLOWING IS KEY TO WHAT WANT PLOTTED
410 PLOT T,B[J,I],-1.5*J
420 NEXT J
430 NEXT I
440 STOP
446 LABEL (*,2.5,1.7,PI/2,6/9)
448 LETTER
450 LABEL (*,2.5,1.7,0,6/9)
451 LETTER
452 END
500 FORMAT F3.0
600 FORMAT F5.2
610 REM: END OF PROGRAM LISTING
```

```
1 REM: PROGRAM TO NUMERICALLY INTEGRATE LAT-DIR EQUATIONS OF MOTION THAT HAVE
2 REM: BEEN REDUCED TO A SINGLE THIRD ORDER ORDINARY DIFFERENTIAL EQUATION
3 REM: IN ONE UNKNOWN.DERIVED FROM LAT-DIR EQUATIONS OF MOTION LESS THE
4 REM: SIDEFORCE EQUILIBRIUM EQUATION. INTEGRATION METHOD USED WAS EULER
5 REM: PREDICTOR-CORRECTOR WITH INTERATION ON CORRECTIONS. EQUATIONS INTEGRAGED
6 REM: CONTAIN INFORMATION ON NONLINEARITY IN YAWING MOMENT AND/OR ROLL/YAW
7 REM: HYSTERESIS.
10 DIM A$[30,30],B$[30,30]
20 DISP "I.C.'S FOR BETA,BDOT,H,L";
30 INPUT B0,B1,H,L
40 DISP "NONLINEAR COEFF.";
50 INPUT E
60 B2=-B0*1.3214*(1+E*B0↑2)
70 DISP "VALUE FOR NR";
80 INPUT N
82 DISP "YAW MOMENT HYSTERESIS";
83 INPUT Y
84 DISP "ROLL MOMENT HYSTERESIS";
85 INPUT R
90 I=J=0
95 REM: BEGIN ITEGRATION
100 FOR K=1 TO 30
110 FOR M=1 TO 30
120 I=I+H
130 IF I>L THEN 330
140 U1=B0
150 U2=B1
160 U3=B2
170 GOSUB 340
180 U4=B3
190 B2=B3*H+B2
200 B1=U3*H+B1
210 B0=U2*H+B0
220 GOSUB 340
230 U5=B3
235 REM: PROGRAM LISTING CONTINUED ON FOLLOWING PAGE
```

```
236 REM: CONTINUED FROM PREVIOUS PAGE
240 B2=((B3+U4)/2)*H+U3
250 B1=((B2+U3)/2)*H+U2
260 B0=((B1+U2)/2)*H+U1
270 GOSUB 340
280 IF ABS(B3-U5)>1E-03 THEN 230
290 A[M,K]=B0
300 B[M,K]=B1
310 NEXT M
320 NEXT K
325 REM: LINK WITH PLOTTING PROGRAM FOR PLOTTING OUTPUT
330 LINK 1
335 REM: EQUATION TO BE INTEGRATED
340 B3=(N-2.4557)*B2-B1*((1.41682-2.4557*N)+3.9642*E*B012)-3.4225*B0
350 B3=B3-3.245*E*B013+2.4557*Y*SGN(B1)+0.0629*R*SGN(B1)
360 RETURN
370 REM: END OF THIS PROGRAM LISTING
```

APPENDIX E

ANALOG COMPUTER PROGRAM FOR

$$\ddot{\beta} = -N_\beta(1 + \epsilon\beta^2)\beta + N_r\dot{\beta} - N_p p + \Delta N * SIGN(\dot{\beta})$$

$$\dot{p} = L_\beta\beta - L_r\dot{\beta} + L_p p + \Delta L * SIGN(\dot{\beta})$$

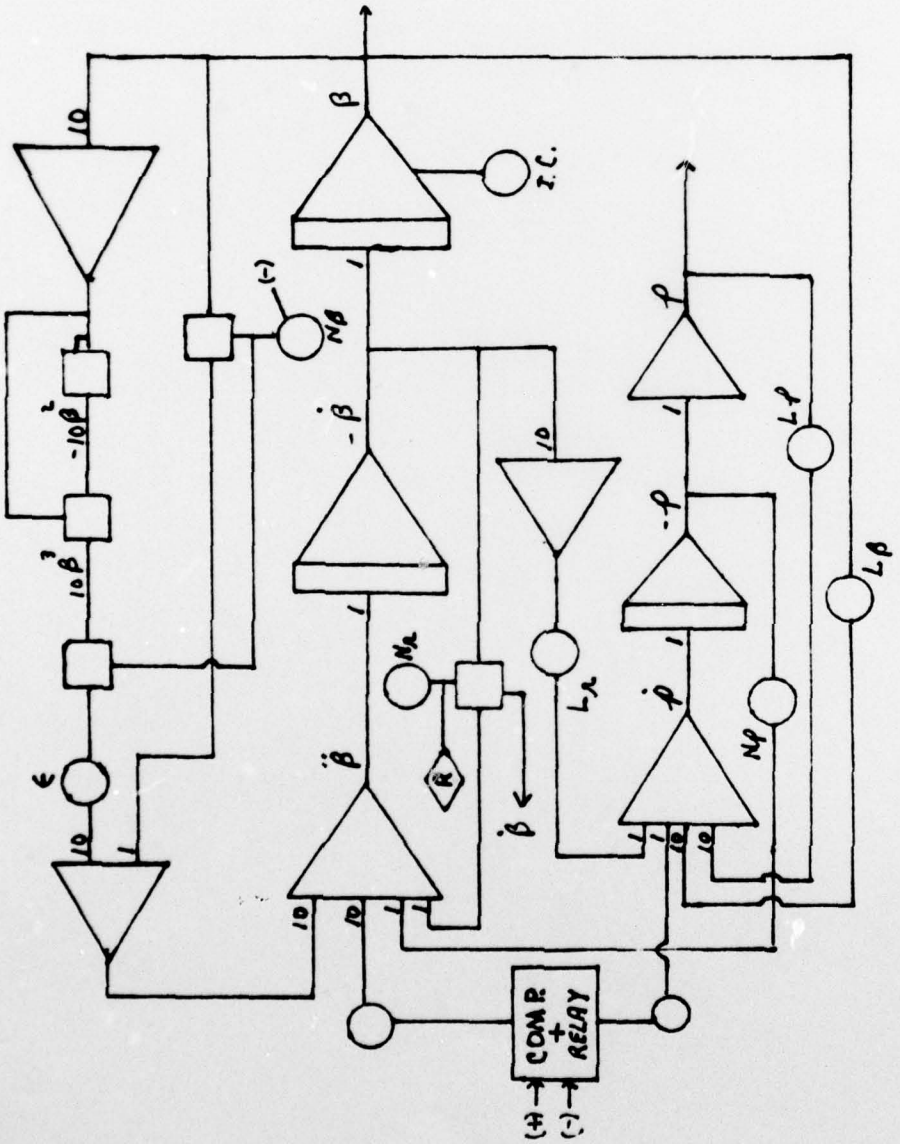

SEE APPENDIX F FOR DEFINITION OF SYMBOLS

APPENDIX F

ANALOG COMPUTER PROGRAM FOR

$$\dddot{B} = -A\ddot{B} - \dot{\beta}(b_1 + 3b_3\beta^2) - c_1\beta - c_3\beta^3$$

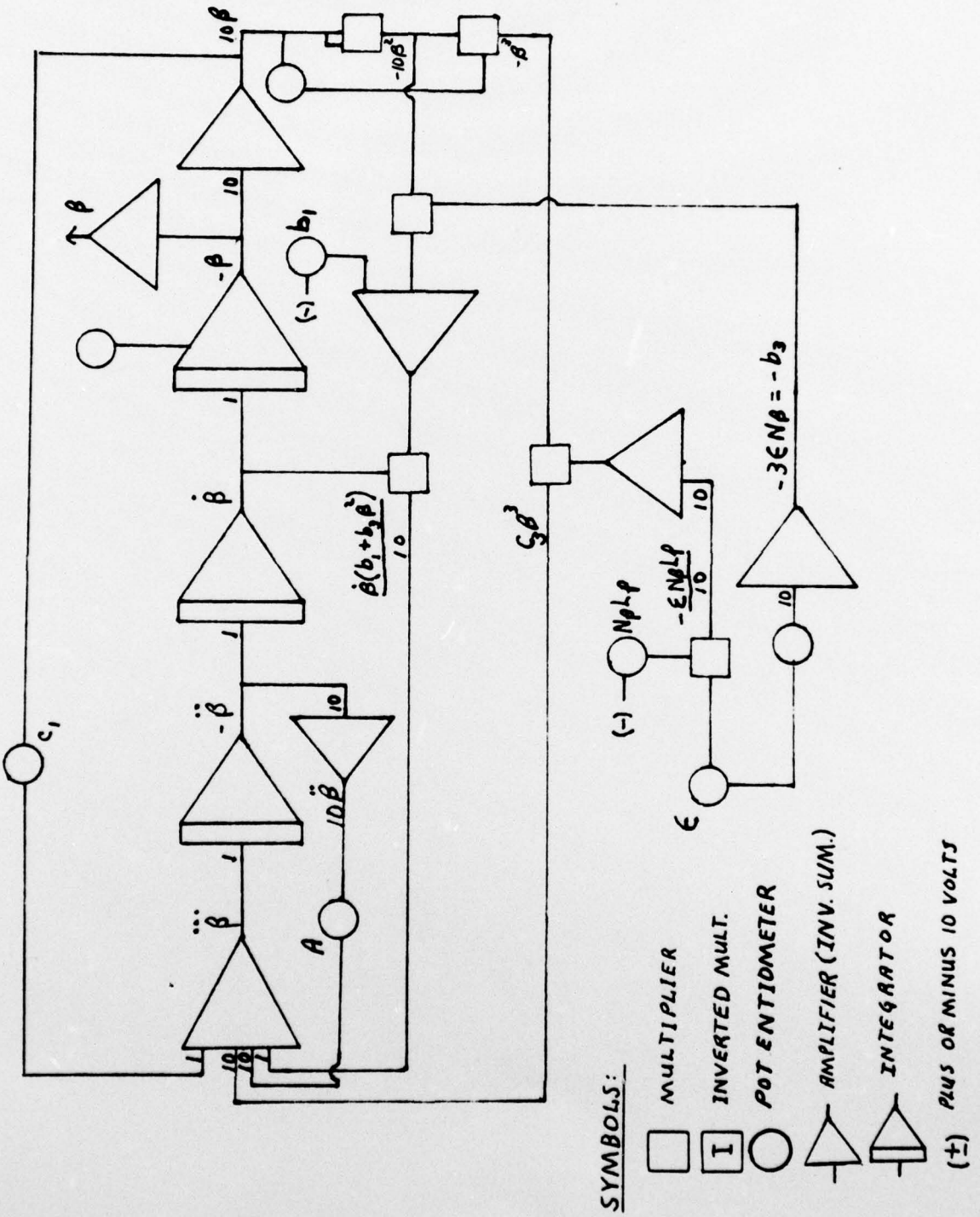

LIST OF REFERENCES

1. Blakelock, J.K., Automatic Control of Aircraft and Missiles, J. Wiley & Sons, 1965.

2. Ottensoser, J., "High Angle of Attack Aerodynamic Data for a 0.10 Scale A-7 Model Evaluated in the 7 by 10 Foot Transonic Wind Tunnel for Investigating the Stall Departure Phenomena, Phase I," NSRDC TM-16-76-16, October 1975.

3. Ross, A.J., "Investigation of Nonlinear Motion Experienced on a Slender-Wing Research Aircraft," Journal of Aircraft, vol. 9, No. 6, September 1972, p. 625-631.

4. Ogata, K., Modern Control Engineering, p. 709, Prentice-Hall, Inc., 1970.

5. Melsa, J.L. and Jones, S.K., Computer Programs for Computational Assistance in the Study of Linear Control Theory, McGraw-Hill, 1973.

6. Gerald, C.F., Applied Numerical Analysis, Addison-Wesley Publishing Company, 1973.

7. Kryloff, N. and Bogoliuboff, N., Introduction to Nonlinear Mechanics, Princeton University Press, Princeton, N.J., 1937.

8. Parkinson, C.U. and Smith, J.D., "The Square Prism as an Aeroplastic Nonlinear Oscillator," Quarterly Journal of Mechanics and Applied Mathematics, vol. XVIII, Pt. 2, 1964, p. 226-239.

INITIAL DISTRIBUTION LIST

		No. Copies
1.	Defense Documentation Center Cameron Station Alexandria, Virginia 22314	2
2.	Library, Code 0142 Naval Postgraduate School Monterey, California 93940	2
3.	Department Chairman, Code 67 Department of Aeronautics Naval Postgraduate School Monterey, California 93940	1
4.	Professor L. V. Schmidt, Code 67Sx Department of Aeronautics Naval Postgraduate School Monterey, California 93940	2
5.	Maj Paul D. Young, USMC 214 Cosky Dr. Marina, California 93933	1